IEEE Journal of Microwaves

Received 28 August 2020; revised 20 October 2020 and 25 October 2020; accepted 26 October 2020.
Date of current version 7 January 2021.

Digital Object Identifier 10.1109/JMW.2020.3035541

The Role of Millimeter-Wave Technologies in 5G/6G Wireless Communications

WEI HONG [1,2] (Fellow, IEEE), ZHI HAO JIANG [1,2] (Member, IEEE), CHAO YU [1,2] (Member, IEEE), DEBIN HOU [1], HAIMING WANG [1,2] (Member, IEEE), CHONG GUO [1] (Graduate Student Member, IEEE), YUN HU [2] (Member, IEEE), LE KUAI [1], YINGRUI YU [1] (Member, IEEE), ZHENGBO JIANG [1] (Member, IEEE), ZHE CHEN [1] (Member, IEEE), JIXIN CHEN [1,2] (Member, IEEE), ZHIQIANG YU [1,2] (Member, IEEE), JIANFENG ZHAI [1,2] (Member, IEEE), NIANZU ZHANG [1], LING TIAN [1,2] (Member, IEEE), FAN WU [1] (Member, IEEE), GUANGQI YANG [1,2], ZHANG-CHENG HAO [1,2] (Senior Member, IEEE), AND JIAN YI ZHOU [1,2] (Member, IEEE)

(Invited Paper)

[1]State Key Laboratory of Millimeter-Waves, School of Information Science and Engineering, Southeast University, Nanjing 210096, China
[2]Purple Mountain Laboratories, Nanjing 211111, China

CORRESPONDING AUTHORS: WEI HONG; ZHI HAO JIANG (e-mail: weihong@seu.edu.cn; zhihao.jiang@seu.edu.cn).

This work was supported in part by the National Key Research and Development Program of China under Grant 2020YFB1804900, in part by the National Natural Science Foundation of China (NSFC) under Grant 61627801, and in part by the High Level Innovation and Entrepreneurial Research Team Program in Jiangsu.

ABSTRACT Ever since the deployment of the first-generation of mobile telecommunications, wireless communication technology has evolved at a dramatically fast pace over the past four decades. The upcoming fifth-generation (5G) holds a great promise in providing an ultra-fast data rate, a very low latency, and a significantly improved spectral efficiency by exploiting the millimeter-wave spectrum for the first time in mobile communication infrastructures. In the years beyond 2030, newly emerged data-hungry applications and the greatly expanded wireless network will call for the sixth-generation (6G) communication that represents a significant upgrade from the 5G network – covering almost the entire surface of the earth and the near outer space. In both the 5G and future 6G networks, millimeter-wave technologies will play an important role in accomplishing the envisioned network performance and communication tasks. In this paper, the relevant millimeter-wave enabling technologies are reviewed: they include the recent developments on the system architectures of active beamforming arrays, beamforming integrated circuits, antennas for base stations and user terminals, system measurement and calibration, and channel characterization. The requirements of each part for future 6G communications are also briefly discussed.

INDEX TERMS 5G communications, 6G communications, antennas, beamforming, calibration, digital arrays, phased arrays, RF integrated circuits, measurement, multibeam arrays, propagation channels, wireless systems.

I. INTRODUCTION

More than a century ago, in the 1890s, the capability of using electromagnetic waves to transmit signals wirelessly was demonstrated, for the first time, in the famous wireless telegraphy experiment conducted by Nobel Laureate G. Marconi [1]. It took around 80 years to turn it into commercial applications with which people can connect each other in real-time. Ever since then, the technologies of mobile communications have evolved rapidly due to the developments in communication theory and multiplexing methods, microelectronics and integrated circuits (ICs), microwave circuits and antennas, and so on [2], [3]. Beginning from the 1980s, a new generation has emerged almost every decade [4]. The first-generation (1G) of mobile communications was based on analog communications by using the frequency-division multiplexing access (FDMA). It only allowed voice signal transfer with limited and unstable spatial coverage [5]. The second-generation (2G) uses digital communications where the time-division multiplexing access (TDMA) and code-division multiplexing access (CDMA) were adopted. The 2G ensured a more stable link, a much wider coverage, and supported text messaging among users [6], [7]. The third-generation (3G) employs variations of advanced CDMA techniques and supports more versatile services, including, for the first time, multimedia data transfer [7], [8]. With the help of orthogonal frequency-division multiplexing (OFDM) and multiple-input multiple-output (MIMO) techniques, the fourth-generation (4G), including the 3.9G long term evolution (LTE) and 4G LTE-advanced was developed. They are able to offer a dramatically faster speed than 3G, providing a data rate of tens of megabytes per second [9], [10]. The revolutionary icon of the 4G era was the burgeoning widespread usage of smart-phones across the world, which changed the life style of human beings and the way people connect with each other. In terms of the frequency spectrums that are designated for the different generations of mobile communications, we can make two observations. First, more frequency bands have been gradually released for a larger channel bandwidth that can meet the demands for higher data rates [5]. Secondly, all the released frequency bands are below 4 GHz, primarily due to two facts: 1) the electromagnetic waves below 4 GHz are less susceptible to blockage and weather changes and 2) the hardware chips and components are more cost-friendly and power-efficient.

With the fast growing of the number of consumer wireless devices in use and the expansion of the Internet of Things (IoT), the amount of mobile data transfer is almost doubled every year, surpassing that of the wired communications [14]. The 4G mobile network infrastructure can no longer meet the needs for high-speed wireless data transmission. Therefore, from the second decade of the 21st century, the fifth-generation (5G) of mobile communications emerges with the outlook to the sixth-generation (6G) [11]–[13]. The 5G has been deployed in 2019 and is on the corner of massive commercialization. The international telecommunication union (ITU) has defined three major application scenarios for 5G new radio (NR): they are the enhanced mobile broadband (eMBB), massive machine type communication (mMTC), and ultra-reliable low latency communication (URLLC) [see Fig. 1]. The 5G is expected to support a data rate of a few gigabits per second (Gb/s), a latency of milli-second, and a high volume of traffic density with greatly improved spectral, energy, and cost efficiencies [15]. In order to meet these requirements, a number of enabling network and hardware technologies have been developed, including ultra-dense networking, all-spectrum access, massive MIMO, and full-duplexing [16], [17].

Importantly, from the frequency resource point-of-view, the uniqueness of 5G, in comparison with 3G and 4G, is the utilization of millimeter-wave (mmWave) frequencies in mobile communications, mainly due to two reasons [18], [19]. First, the sub-6 GHz spectrum has already been very crowded, filled

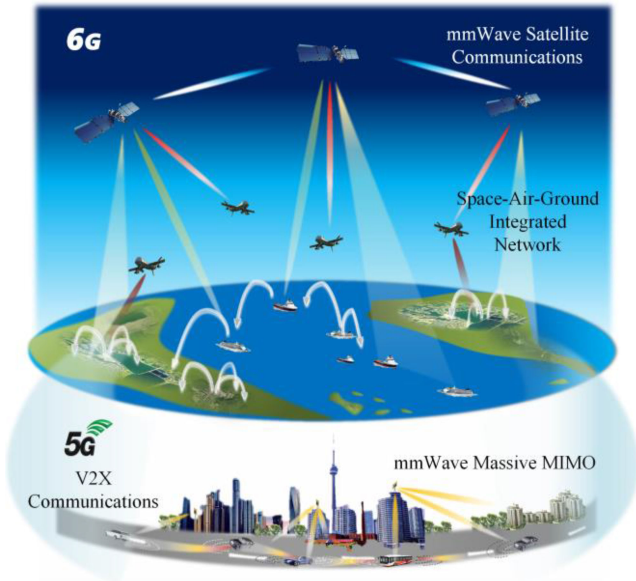

FIGURE 1. Conceptual illustration of the 6G communication network that encompasses the 5G network.

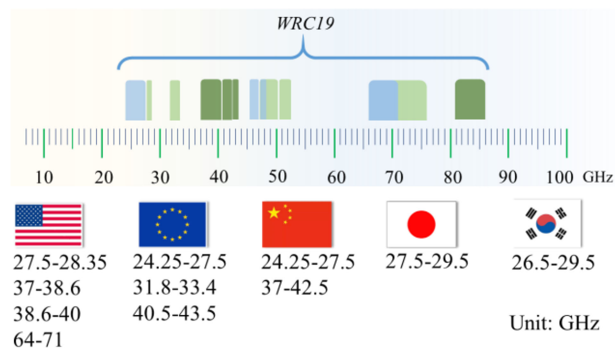

FIGURE 2. The mmWave 5G bands released by different countries.

with distributed bands dedicated for cellular communications, satellite and aerial communications, and wireless local area networks (WLANs). On the contrary, at mmWave frequencies from 6 GHz up to 300 GHz, there are many unlicensed bands – the available spectrum is abundant. Secondly, the absolute bandwidth at mmWave frequencies is much larger than that at the lower microwave frequencies under the same relative bandwidth. The Third Generation Partnership Project (3GPP) has divided the 5G New Radio (NR) into FR1 band, i.e., 410 – 7125 MHz, and FR2 band, or also called mmWave band, i.e., 24.25 – 52.6 GHz [20]. In addition to the narrow bands around 3.5 GHz and 4.9 GHz, many countries have released a number of mmWave bands for 5G NR communications in the *Ka*-band, *Q*-band, and even *E*-band [see Fig. 2] [22]. Consequently, the system architecture, transceiver channels, ICs, passive and active components, and propagation channel modeling have become the main cutting edges of research [23]–[26].

Moving towards 2030 and beyond, due to the fast growth of new technologies such as virtual reality, vehicle-to-X network, unmanned aerial vehicle network, mid-earth-orbit (MEO) and low-earth-orbit (LEO) satellite network, and oceanic information network, the 5G communications would become insufficient. Therefore, very recently, several countries have called for or initiated research programs for the sixth generation (6G) of mobile communications. Although the specs of 6G, such as frequency bands, data rate requirements, have not been defined and finalized, its applications have been considered. A consensus for 6G has been reached – the 6G will be an intelligent mobile communication network of a much larger scale that encompasses the 5G [13], [27]. While the quasi-two-dimensional 5G network only covers a limited portion of lands on earth, the 6G network will extend into three dimensions and connects the satellites, aircraft, ships, and land-based infrastructures, providing a truly global coverage. The mmWave technologies will play an important role in enabling the various wireless links with enhanced speed and reliability superior to 5G. In addition, the use of terahertz has also been proposed as a part of the frequency bands for 6G communications [27]. However, the related key devices of terahertz chips, front-end components, and systems are not yet as mature and reliable as those operating at mmWave frequencies for long-distance communications with a high fidelity.

In this paper, the mmWave technologies that are important to 5G communications are reviewed, including the massive MIMO system architectures, beamforming chips, antennas for base stations (BSs) and user terminals (UTs), system measurement and calibration techniques, and wireless channel characterization. Then, the challenges and requirements for future 6G communications are discussed. The paper is organized as follows. Section II illustrates the system architectures of active multibeam arrays, including a comparison among different beamforming strategies. In Section III, the mmWave chips for beamforming are presented. The mmWave antennas for both BSs and UTs are described in Section IV, along with a discussion on several advanced antenna technologies. In Section V, the methods for system calibration and pattern measurement, RF testing, and system performance testing are reported. Section VI presents a brief overview of channel characterization, followed by conclusions drawn in Section VII.

II. mmWAVE SYSTEMS FOR 5G/6G COMMUNICATIONS

To overcome the large free-space path loss of the radiated waves at mmWave frequencies, beamforming techniques have been widely employed in 5G wireless systems for effectively focusing the radiated energy into the targeted directions. As shown in Fig. 3, the general architecture for a 5G mmWave BS is illustrated, including the active antenna units (AAUs), the baseband units (BBUs), and the core network (CN). The beamforming AAU contains an antenna array, down/up converters, analog-to-digital converters (ADCs), digital-to-analog converters (DAC), beam management units, and AAU baseband signal processing units. To realize the desirable beamforming functions, proper amplitude and phase should be assigned to each antenna element. In this section, several mainstream beamforming architectures will be described and compared, followed by a discussion on potential system architectures for 6G systems.

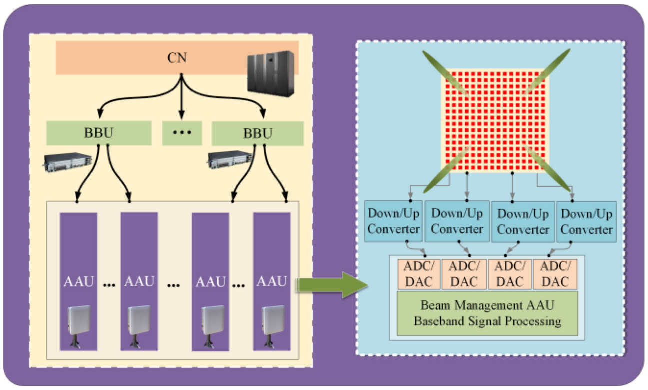

FIGURE 3. An illustration of the system architecture of a 5G base station.

A. SYSTEM ARCHITECTURE

Based on the methods to phase each antenna element, we can divide beamforming architectures for 5G wireless systems into three types: analog beamforming [28]–[37], full-digital beamforming [38]–[40], and hybrid beamforming [41]–[46] [see Fig. 4].

Due to its low-cost and implementation convenience, the analog beamforming has been widely employed, in which phase shifting is realized in the analog domain, as shown in Fig. 2(a). Depending on the location of the analog phase shifting performed in the system, it can be categorized into intermediate frequency phase shifting [31], local oscillator (LO) phase shifting [28], and radio frequency (RF) phase shifting [32], [33]. The phase-shifting can be realized by utilizing digitally-controlled phase shifters, such as a 6-bit phase shifter, or static analog beamforming structures, such as the Butler matrices [34], Blass matrices [35], and lenses [36]. It is worth mentioning that the phase shifter is one of the most popular schemes in commercial beamforming chips, in which the digital control of phase shifting can be pre-calibrated and stored in the memory for fast and precise beam generation. For example, a *Ka*-band phased array antenna with 64 radiating elements based on quad-core monolithic microwave ICs (MMICs) has been demonstrated, as shown in Fig. 5 [37].

Compared with the analog beamforming, the full-digital beamforming possesses more flexibility. As shown in Fig. 4(b), each antenna is directly connected to a transceiver chain, followed by an ADC/DAC with a high sampling rate and precision. A *Q*-band 64-channel full-digital beamforming transceiver for 5G communications has been proposed and implemented [40], covering a frequency range from 37 to 42.5 GHz [see Fig. 6]. Due to the employed digital circuit, this kind of beamforming structure can realize a high beamforming performance, especially for multi-beam radiation and reception. However, the cost of hardware implementation and

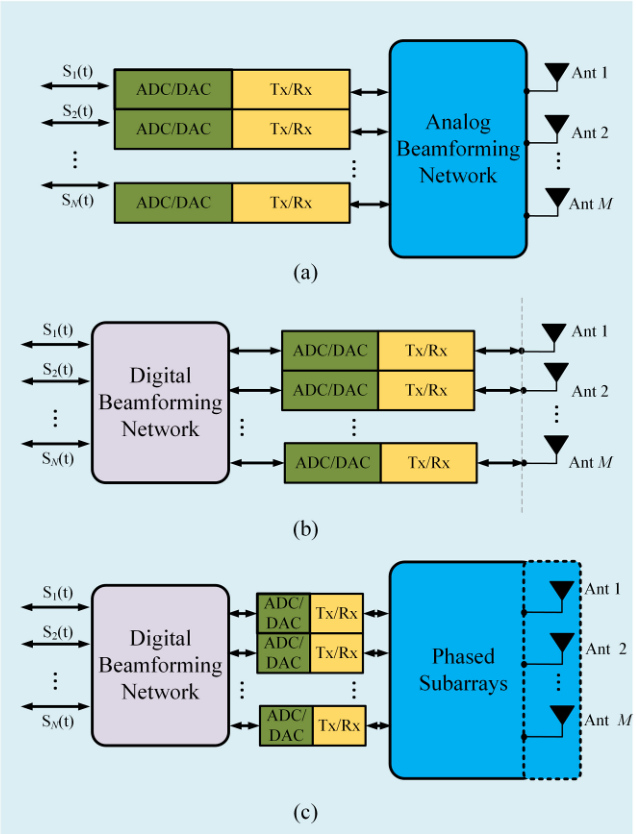

FIGURE 4. **Illustrations of the different beamforming system architectures: (a) analog beamforming, (b) full-digital beamforming, and (c) hybrid beamforming.**

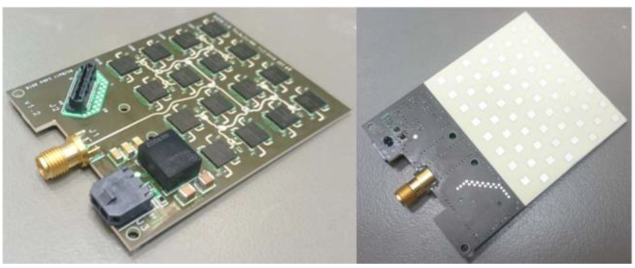

FIGURE 5. **Photographs of a *Ka*-band analog beamforming array module based on phase shifting chips (reproduced from [37]).**

FIGURE 6. **Photographs of Q-band digital beamforming array modules [40].**

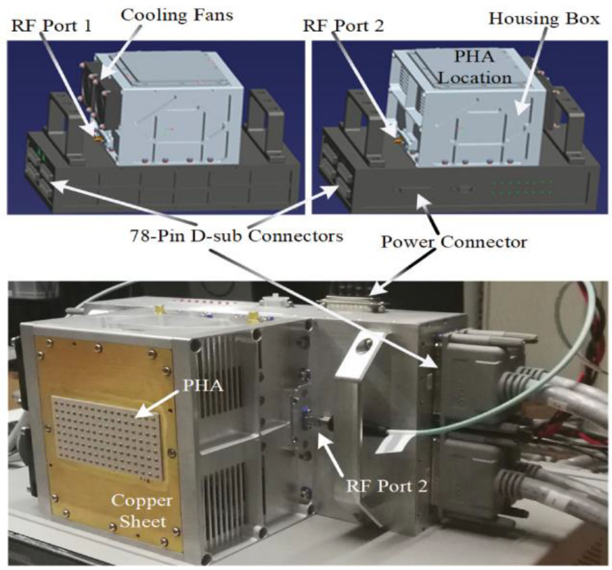

FIGURE 7. **Photographs of a prototype of the hybrid beamforming array (reproduced from [44]).**

the burden of signal processing in the baseband will increase very quickly as the channel number increases or the channel bandwidth broadens, limiting its commercialization.

To realize the trade-off between system performance and hardware complexity, the hybrid beamforming structure was proposed and has been widely applied in the development of commercial active antenna units (AAUs), as shown in Fig. 4(c). In [44], the authors presented a hybrid beamformer consisting of two RF channels connecting to the baseband and a 128-element antenna array [see Fig. 7]. In such a structure, the phase distribution is realized in both the digital and analog domains, leading to a significant reduction in the number of RF chains.

Currently, the 5G wireless communication systems mainly adopts the hybrid beamforming scheme. Depending on the application scenarios, the BSs [47] and UTs [48] usually have different requirements. For the BSs, massive MIMO can be deployed to obtain satisfactory equivalent isotropically radiated power (EIRP), in which the circuit architectures should be designed by considering the power level. For example, for a medium EIRP, the multi-channel beamforming ICs with antenna-in-package (AIP) technologies [49] can be used for achieving a high level of integration. However, for large EIRP requirements, additional power amplifiers with advanced processing technology can be employed, such as GaN [50]. For the UT, to achieve high-density integration and low power consumption, AIP or antenna-in-module (AIM) [51] technologies are preferable. Besides, to obtain a broad spatial coverage, many AIPs or AIMs are required to be integrated together. In general, such hybrid beamforming structures can have a satisfactory performance with relatively lower complexity, enabling large scale deployment. It is worth noting that, in the current mobile communication market, a radio system is usually supplied by a single company, making it difficult to interface with the systems or components provided by any other third party. To address this issue, the concept of the open radio access network (O-RAN) has been proposed recently [52]. It allows for open interfaces for 5G equipment, aiming at establishing a healthier eco-system for 5G communications.

B. POTENTIAL SYSTEM ARCHITECTURE FOR 6G COMMUNICATIONS

To further extend the capability of communication systems, the concept of 6G has recently emerged [13]. The purpose of from 1G to 5G is to build wireless connections among people, mainly in the terrestrial land areas or environments. However, most of the areas on the earth are oceans, deserts, and the near outer space. The 6G is intended to cover these areas and support an integrated ground-air-space network [53], covering the entire earth's surface and near outer space. Several pioneered companies have initiated projects for enabling networks of such kind, including SpaceX [54], Amazon, and OneWeb [55].

To meet the demands for 6G communications, future wireless systems need to be reconfigurable [56] and intelligent [57]. The reconfigurability should include system hardware re-uses and mode-switching. Meanwhile, with the rapid development of artificial intelligence [57], [58], such as machine learning [59], a 6G system is also required to be intelligent for providing better services, including the adaptation to environments and changes of functionality.

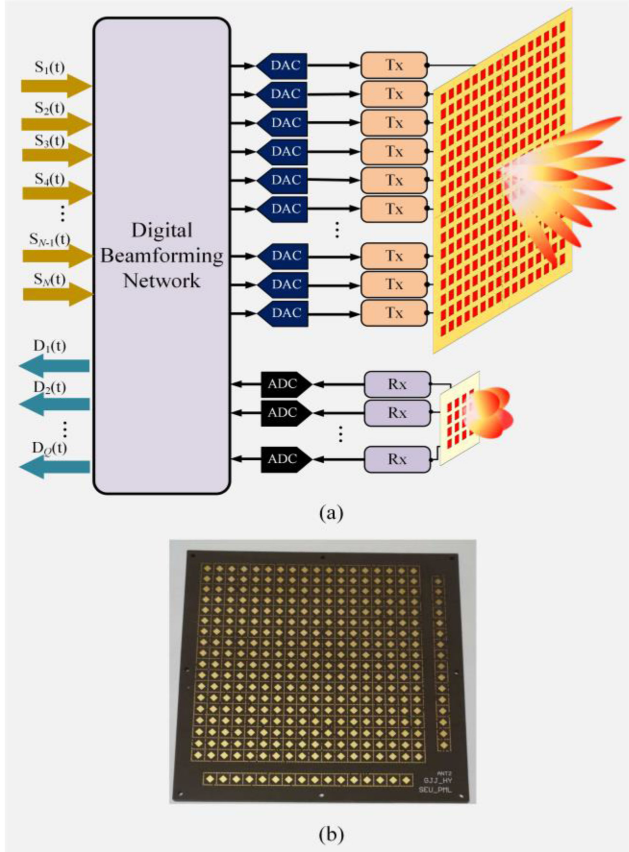

FIGURE 8. (a) System architecture and (b) a prototype photograph of the asymmetric beamforming arrays.

C. SYSTEM REQUIREMENTS FOR ASYMMETRICAL WIRELESS SYSTEM

Conventionally, the transmitter and receiver antenna arrays are reciprocal. However, from the system point of view, this is not necessary since the transmitter and receiver could have different requirements and functionality, depending on the specific application scenarios. Therefore, asymmetric architecture is an alternative option for future designs, resulting in a better efficiency and lower cost and complexity.

In order to incorporate the asymmetric property into a full-digital array, a novel transmitting and receiving beamforming strategy was proposed recently [60], in which nonreciprocal beamforming was developed. It achieves the asymmetrical transmitting and receiving beam patterns, as shown in Fig. 8(a). The general goal of such a structure is to reduce both the hardware and baseband resource consumption while keeping the salient properties of the full-digital arrays. As a proof-of-concept validation on the proposed system structure, an asymmetrical full-digital array prototype was developed as shown in Fig. 8(b). It can be seen that the Tx array employs 16×16 full-digital channels surrounded by dummy elements, while the Rx array only contains two sets of 1×16 full-digital channels. Compared with the conventional arrays having the same number of transmitting and receiving channels, this leads to a significant reduction in hardware resources, power consumption, and signal processing. For such a system, the transmitting and receiving beams can still possess a broad coverage with a high degree of beamforming flexibility.

To appreciate the advantages of the proposed architecture, a performance comparison among different beamforming array structures is listed in Table 1. The asymmetrical full-digital array has properties similar to those of a conventional symmetrical one, such as broad instantaneous coverage, low complexity, and high system capacity. The complexity and cost of system implementation, as well as the total power consumption are greatly reduced. In short, asymmetrical full-digital array poses as one of the most promising candidates for 6G communication systems. It will present different design requirements and challenges for beamforming ICs, transceiver channels, and antenna arrays.

III. mmWAVE BEAMFORMING CHIPS FOR 5G/6G COMMUNICATIONS

Silicon based mmWave chips are one of the main solutions for current 5G mmWave arrays and are also one of the most competitive technologies for 6G mmWave arrays. In this section, typical architectures of mmWave chips for hybrid massive MIMO and the performance of currently available commercial TRx beamformer chips are described. In addition,

TABLE 1. Comparison Among Different mmWave Beamforming System Architectures

System Architecture	Instantaneous Coverage	Complexity of Beam Management	Number of Simultaneous beams	System Capacity	Complexity of System Implementation	Cost	Complexity of Data Processing	Power Consumption
Hybrid Array	Narrow	Medium	Small	Medium	Low	Low	Medium	Medium
Symmetrical Full-Digital Array	Wide	Low	Large	High	High	High	High	High
Asymmetrical Full-Digital Array	Wide	Low	Large for downlink, medium for uplink	High for downlink, medium for uplink	Medium	Medium	Medium	Medium

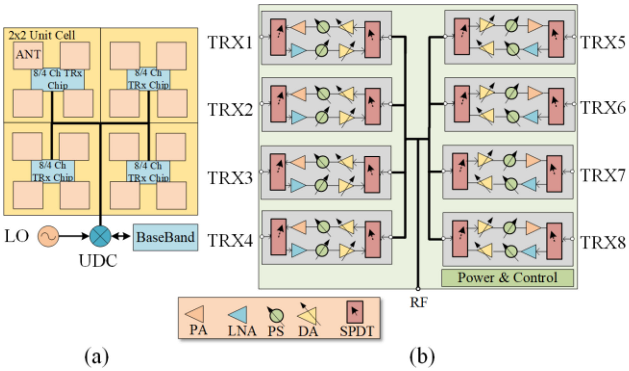

FIGURE 9. (a) Architecture of a 16-element 4-cell 5G hybrid massive MIMO array module based on 8/4 Tx/Rx beamformer chips. (b) Block diagram of an 8-channel TRx beamformer chip.

potential chip architectures for asymmetrical massive MIMO systems are also discussed.

A. mmWAVE CHIPS FOR HYBRID MASSIVE MIMO

A typical hybrid massive MIMO array chipset is shown in Fig. 9(a), which is composed of 16 antennas, one intermediate frequency (IF) channel, and one baseband channel. It includes 8/4 multi-channel beamformer chips and one up/down converter (UDC) chip that connect to the IF and baseband channel.

Depending on the type of antenna elements (single- or dual-polarized), 4-channel or 8-channel TRx beamformer chips should be used to support a subarray of 2 × 2 elements. The current 8/4-channel TRx beamformer chip's function is to adjust each RF channel's phase and amplitude. [61] presents the basic functions of beamformers that have been commercialized in industries. Fig. 9(b) shows a simplified block diagram of the 8-channel TRx beamformer chip. A single Tx chain contains a PA, a digitally-controlled phase shifter, and an attenuator. A single Rx chain contains a low noise amplifier (LNA), a digitally-controlled phase shifter, and an attenuator. RF switches are used to switch the operation mode in a time-division duplex (TDD) based communication system. In order to combine all the signals from the TRx channels, the beamformer also contains a power combining/splitting circuit inside the chip.

Many early works used different manufacturing processes such as SiGe, CMOS, and SOI, with the channel numbers ranging from 4 to 32 [47], [62]–[64]. For industrial applications, most of the chips use SiGe process containing 4 channels for single-polarized antennas and 8 channels for dual-polarized antennas. Table 2 lists some commercially available TRx beamformer chips and their performance parameters are available in the public domain. Fig. 10 shows a photograph of a packaged 8-channel TRx beamformer chip using the WLCSP package from MISIC microelectronics.

The UDC chips are used to interface the baseband circuits by performing frequency conversion between RF and IF. Fig. 11 shows the block diagram of a UDC chip. The UDC chip contains an up converter and a down converter. In the down converter, the received RF signal will be filtered with its amplitude controlled. Then the signal will be converted to IF I/Q signal for baseband processing. In the up converter, the IF I/Q signal generated at the baseband will be converted to RF. Then, it will be filtered with its amplitude controlled to interface with RF beamformer chips.

B. mmWAVE CHIPS FOR ASYMMETRICAL MASSIVE MIMO SYSTEMS

For asymmetrical massive MIMO systems, since the signal from each antenna element will be processed in the baseband, the signal combining/splitting circuit can be eliminated. Hence, the block diagram of multi-channel mmWave chips for asymmetric wireless systems is different from that for the hybrid massive MIMO array systems.

Fig. 12(a) shows the architecture of a Tx array module with 16 antennas elements. The chipsets include four 4-channels with an up converter for each channel inside the chip. The number of IF channels is equal to that of the RF channels. Fig. 12(b) shows an asymmetrical Rx array module containing 8-antenna elements. The chipsets include two 4-channel chips with down converters inside.

Figs. 13(a) and (b) show the block diagrams of multi-channel Tx and Rx chips with mixers for asymmetrical massive MIMO arrays. While the Tx chain contains the typical transmitter circuits including mixers, filters, PAs, *etc.*, the

TABLE 2. Some Commercial TRx Beamformer Chips

Vendor Name	ADI	Anokiwave	IDT	NXP	MISIC
Process	SiGe BiCMOS	SiGe BiCMOS	SiGe BiCMOS	SiGe BiCMOS	SiGe BiCMOS
Channel Number	16	4/8	4/8	4	4/8
Frequency (GHz)	24 – 29.5	26.5 – 29.5	25 – 30	26.5 – 29.5	24.25 – 27.5
Tx P1dB (dBm)	--	15-18	12-16	19	17
Noise Figure (dB)	--	--	5.5	6	5
Memory	--	512	2048	--	512
Package	LFCSP	WLCSP	WLCSP	WLCSP	WLCSP

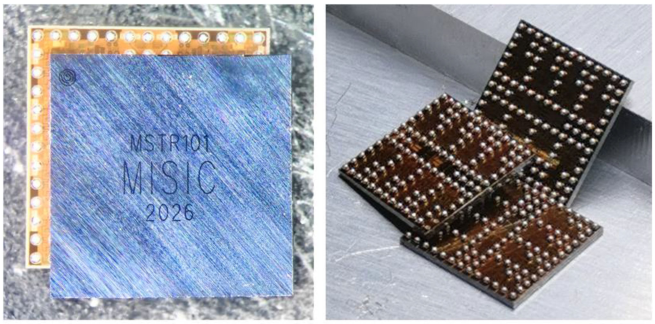

FIGURE 10. Photographs of the 8-channel TRx beamformer chips with WLCSP package from (courtesy of *MISIC*).

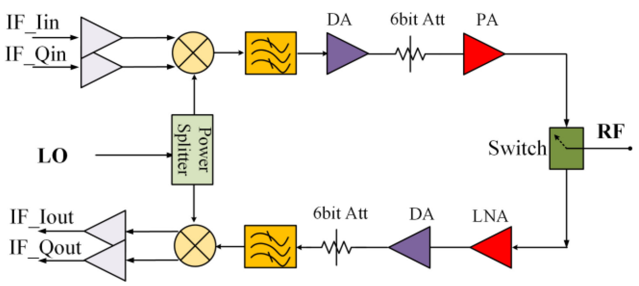

FIGURE 11. Block diagram of a UDC chip.

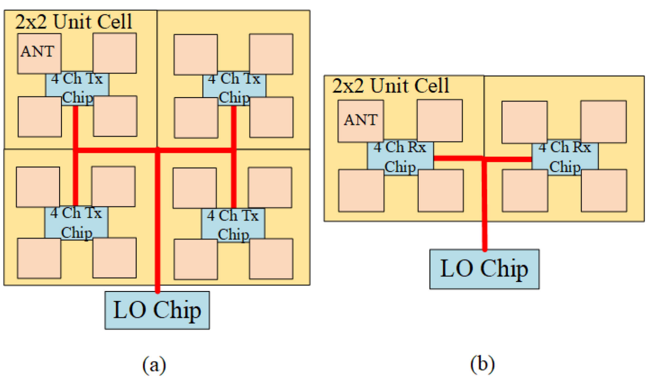

FIGURE 12. (a) The architecture of a 16-element 4-cell asymmetrical massive MIMO Tx array module based on four 4-channel chips with mixers inside. (b) The architecture of an 8-element 2-cell asymmetrical massive MIMO Rx array module based on two 4-channel Rx chips with mixer inside.

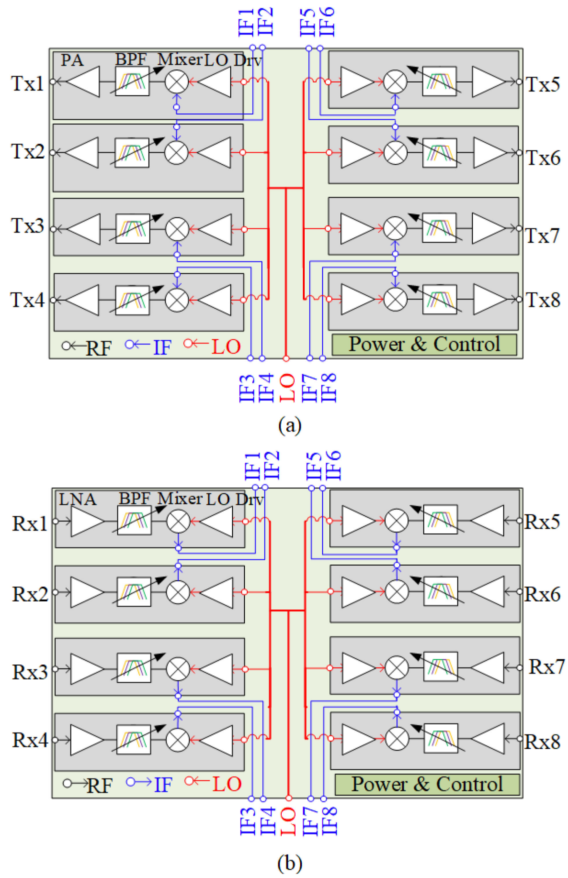

FIGURE 13. Block diagrams of (a) a multi-channel Tx chip with mixers and (b) a multi-channel RX chip with mixers for asymmetrical massive MIMO arrays.

Rx chain has the typical receiver circuits including mixers, filters, LNAs, *etc*. Multi-channel IF signals are used to interface with the baseband. The multi-channel Tx and Rx chips could be used to implement asymmetrical massive MIMO arrays described in sub-Section II.C with different scales.

IV. mmWAVE ANTENNAS AND MODULES FOR 5G/6G COMMUNICATIONS

Antennas are critical front-end passive components that are responsible for emitting and receiving electromagnetic waves in wireless communication systems [65]. Their electrical properties, including the input impedance, radiation pattern, gain, polarization, and passive intermodulation, will affect the signal coverage, efficiency, noise figure, and linearity of the system. For 5G communications, the system requirements call for new broadband/multiband and fully-integrated mmWave antennas with dual-polarization and wide beam coverage [22], [66]. Therefore, extensive efforts have been made on mmWave antennas for 5G BSs and UTs in academia and industry. In this section, the recently developed state-of-the-art mmWave antennas and related advanced technologies will be discussed.

A. mmWAVE ANTENNAS FOR 5G BSS

For 5G BSs, large antenna arrays with a large number of elements are required. It can provide a high degree of freedom for achieving flexible beamforming [67]. In the sub-6 GHz frequency range, $\pm 45^\circ$ dipole antennas with vertically assembled balun circuits are commonly used as dual-polarized radiating elements for BSs [68]. Conventionally, an antenna is usually designed and fabricated and then connected to the RF front-end modules using cables. However, such a process is no longer suitable for massive MIMO arrays at mmWave frequencies, since phase and amplitude variations caused by the cables and connectors among a large number of channels could be significant. For 5G BSs, the antenna array and the RF front-end circuits need to be fully integrated and jointly designed [69].

In addition, a wide and stable beamwidth that can be supported within one or more issued 5G mmWave frequency bands is much desirable. So far, several types of mmWave antennas for BS applications have been proposed, including the tapered slot antennas fed by substrate integrated waveguides (SIWs) [70], magneto electric dipoles [71], vertically-folded patches [72], metasurface radiators [73], aperture radiators [74], and so on. However, they do not have dual-polarization, which limits their applications in 5G BSs.

More advanced dual-polarized antenna elements have also been proposed, with circular patches [75], cavity-backed shorted patches [76], and crossed slots [77]. They have the advantages of being low-profile and low-cost. But their bandwidth is only about 10%, which is not wide enough to cover the 5G bands at *Ka*-band and *Q*-band. To further extend the bandwidth, stacked patches [37], magneto-electric dipoles fed by SIWs [78], and stacked patches with shorting pins and parasitic elements [79] were proposed. They can achieve a matched impedance bandwidth of about 20% with a stable pattern. Moreover, by exciting multiple characteristic modes in a metasurface with non-uniform unit cells, dual-band was realized that simultaneously covers the 5G bands at *Ka*-band and *Q*-band [80]. In addition, antenna elements that support dual-circularly-polarized radiation have also been proposed based on a dual-layer SIW structure with broken mirror symmetry at the SIW open ends [81].

Other techniques for achieving multibeam antennas using passive structures have also been considered. These include the circuit-based Butler matrix beamformer [82] and quasi-optical architectures using multi-feed lenses [83], [84]. Although the generated beams are static with each beam pointing in a pre-defined direction, these antennas are low-cost and light-weight and are useful in certain application scenarios.

B. mmWAVE ANTENNAS FOR 5G UTS

Different from the antennas for BSs, although beamforming is still necessitated at UTs, the number of elements is lower due to the limited space. Antennas operating in the sub-6 GHz frequency regime have been investigated for more than 20 years [85], however, the integration of mmWave antennas and arrays into UTs is a developing field. In addition to the general requirements of antennas, the UT platform requires special design considerations as follows [86].

First, it is preferable that the mmWave antennas are fully incorporated inside a UT. In detail, the antenna structures should not protrude out of the periphery of a cellphone for achieving better mechanical protection of the antennas and having an exterior friendly to the users.

Secondly, the arrays of mmWave antennas should cover as much as possible the entire sphere with an EIRP greater than a certain threshold since the orientation of mobile phones are constantly changing in realistic scenarios [87]. Such a signal coverage is characterized by the coverage efficiency, which describes the spatial coverage of an antenna array with scanned beams [88]. Due to the sub-hemispherical beam steering coverage of planar phased arrays, in order to obtain a high coverage, multiple sets of arrays need to be employed on a UT and their locations have to be optimized.

Thirdly, the user influence needs to be taken into consideration [89]. Due to the small form factor of mmWave antennas, the human body, such as hands in close proximity to the mmWave antennas, would dramatically change the antennas' electrical properties. It can cause severe impedance mismatch, pattern distortion, and radiation efficiency degradation.

Finally, the integration of antennas and RFICs is another critical issue [90]. For a UT such as a smart phone, it is very likely that it will carry more and more sensors which require space to install. Consequently, the seamless connection between the RFICs and the antenna arrays to form an integrated front-end mmWave module not only saves the precious space in a UT but also improves the overall system performance.

Ever since the mmWave antennas for cellular handsets reported was reported in 2014 [91], much research so far has been focused on tackling the above issues. Numerous new antenna designs, layout strategies, and packaging architectures for UT platforms have been proposed and investigated. In terms of radiation mechanisms, they can be classified into two types: one utilizes end-fire radiators, while the other employs broadside radiators. In the case of cellular phones, due to the geometrical shapes, end-fire antennas are the favorite. They can be integrated into the multilayer circuit board inside the handset frame and radiate out from the sidewalls. The vertically-polarized end-fire antenna elements have been proposed by using SIWs with open ends [92], monopoles with

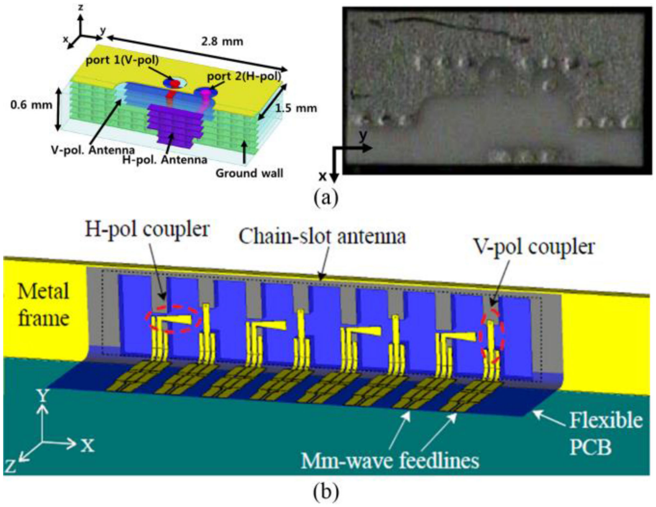

FIGURE 14. Dual-polarized end-fire antennas for UTs based on (a) LTCC technology (reproduced from [102]) and (b) flexible printed circuit boards (reproduced from [103]).

parasitic elements [93], magneto-electric dipoles [94], cavity-backed slots [95], and folded slots [96]. The horizontally-polarized mmWave end-fire antennas for UTs have been realized with Yagi-Uda radiators [97], asymmetrical twin dipoles [98], *etc*. In contrast, broadside radiators have been less studied, primarily attributed to their limited application due to the radiation angular coverage with respect to the array board. Arrays of patches and slot radiators [99] have been implemented. They are placed on the top and bottom facets or vertically attached to the bezel regions of a handset. Efforts have also been made to exploit designs that do not require cutting a window out of the metallic frame of the handset. Rather, only narrow slots need to be etched out for allowing horizontally-polarized radiated waves passing through to the outside space [100].

Recently, the research in the area has focused on designing dual-polarized antennas and arrays for UTs. In [101], a vertically-polarized open cavity and a horizontally-polarized Yagi-Uda radiator was combined to offer dual-polarized end-fire radiation from 34 to 38 GHz. Based on the low-temperature cofired ceramics (LTCC) process, as shown in Fig. 14(a), a folded slot and a via-strip based mesh-grid patch was realized for achieving dual-polarized radiation at 60 GHz [102]. By utilizing the SIW structure, two dual-polarized end-fire radiating elements and their arrays were designed – one is based on the magneto-electric dipole concept [103] while the other is enabled by jointly exploiting the open waveguide and periodic plate loading [104]. In [105], as shown in Fig. 14(b), a chain-slot structure cut out on the frame of the cellular handset, which is fed by vertical and horizontal probes, was used to achieve dual-polarized end-fire radiation with the beam steering capability. The advantage of this design lies in the fact that the chain-slot does not break the integrity of the frame, which makes possible the co-location of the sub-6 GHz and mmWave antennas in the same volume.

Several research reports described the impact of the user body on the antenna performances and thus the data rates. It has been shown that at mmWave frequencies, the effect is much more significant than that at microwave frequencies [106]. Through simulations and measurements of the signal coverage of array antennas deployed at different positions on a UT with different orientations, it was found that at least two arrays are required to mitigate the hand effect [107]. More than three sets of arrays were considered recently – they are placed on the top and the sides of a cell phone.

C. ADVANCED mmWAVE ANTENNA TECHNOLOGIES

Due to the stringent requirements on the antenna bandwidth, module integration, and unconventional operating platform, advanced antenna concepts and technologies have emerged and been investigated. It should be noted that the successful realization of high-performance antenna arrays depends on the radiators' structural designs and as well as materials, packaging, inter-connections, and many other factors. Here, several related antenna concepts and technologies are briefly discussed.

1) INTEGRATED FILTENNAS

The 5G communication systems are "band-pass" systems that require band-pass filters embedded in the front-end circuits to eliminate interference due to the out-of-band signals. The conventional approach is to cascade an antenna and a band-pass filter, each matched to a common purely real input impedance. However, this would result in a large device footprint and a degraded impedance matching over a wide bandwidth. In recent years, the concept of integrating an antenna and a band-pass filter into a single component, referred to as "filtenna", has garnered a lot of attention [108]–[111].

The filtenna has an S_{11} similar to that of a band-pass filter, while its frequency-dependent gain curve resembles the shape of the S_{21} curve of the band-pass filter. Three strategies have been used in designing filtennas. The first one involves adding a band-pass filtering structure in front of the radiator without increasing the form factor of the resulting component, such as a horn antenna integrated with a frequency selective surface placed right at the horn aperture [108]. The second method treats the radiator as the last resonator in a coupled-resonator band-pass filter [109], [110]. In such a way, the operational bandwidth of the original narrowband radiator can be greatly broadened and a sharp roll-off can be achieved in the gain response. It can have both linear-polarization and circular-polarization. The last approach utilizes embedded resonant structures within the radiator, thereby forming radiation nulls for realizing the filtering response [111]. Recently, a broadband mmWave filtenna has been proposed and demonstrated, which can be useful candidates for 5G systems [79].

2) SUB-6 GHZ AND mmWAVE DUAL-BAND ANTENNAS

Since both sub-6 GHz and mmWave bands are expected to be used for 5G communications, shared-aperture antennas

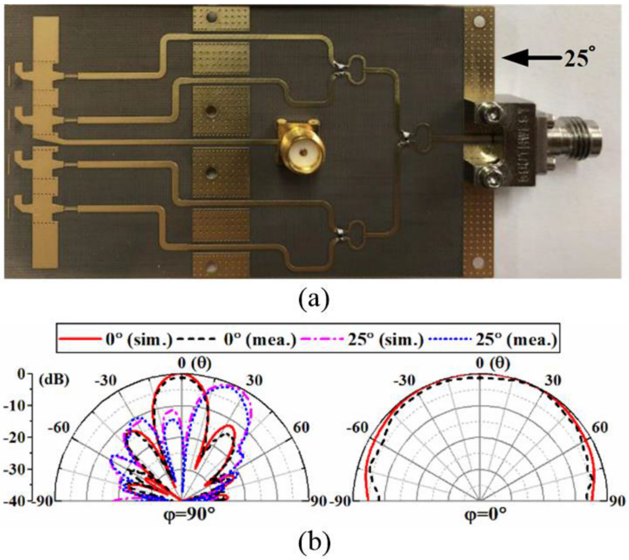

FIGURE 15. **(a) A photograph of the prototype of a sub-6 GHz and *Ka*-band shared-aperture end-fire antenna based on SIW structures and (b) simulated and measured radiation patterns at 26 GHz and 3.5 GHz (reproduced from [114]).**

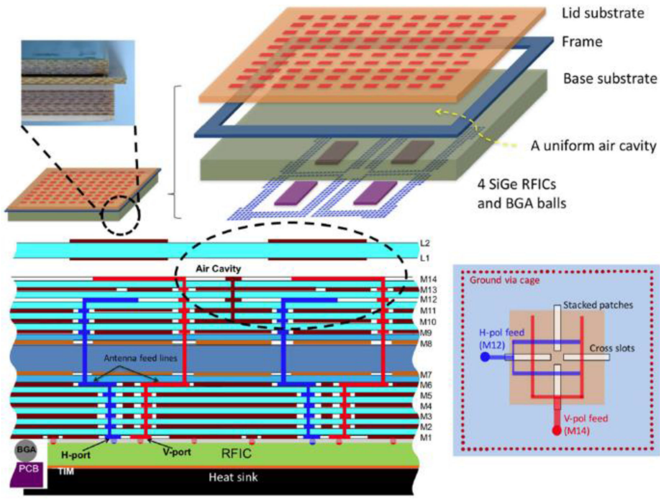

FIGURE 16. **Configuration of a *Ka*-band phased array antenna module (reproduced from [122]).**

that simultaneously support the operation at both microwave and mmWave bands have recently emerged. There is a considerable frequency difference between the two bands and, therefore, the dimension requirements at the two bands are different for the antennas. For example, a single patch element operating at 3.5 GHz occupies an area similar to the size of an array containing about 8 by 8 elements radiating at 28 GHz. On the one hand, the metallic structure of the low radio frequency radiator, which is electrically large at mmWave frequencies, can be utilized as the platform to contain mmWave arrays. On the other hand, the radiating structures working at mmWave frequencies, which are relatively small in size, will not strongly affect the proper operation of the antennas radiating in the sub-6 GHz bands.

By taking advantage of such structure-reusable properties, several broadside and end-fire coexist designs of sub-6 GHz and mmWave antennas have been proposed and demonstrated. By incorporating various types of SIW slot arrays [112] and partial reflective metasurface radiators [113] into a modified patch antenna, broadside radiation at the sub-6 GHz 5G band and a high gain or steerable beam at the mmWave 5G band can be simultaneously achieved. As shown in Fig. 15, by embedding an array of SIW-fed dipoles into a low-frequency dipole, end-fire radiation can be obtained simultaneously at 3.5 and 28 GHz [114]. Alternatively, by embedding SIW transverse slot arrays into planar monopole-like multi-mode low-frequency radiators [115], omnidirectional and unidirectional radiation can be achieved at microwave and mmWave 5G bands, respectively. By utilizing the metallic frame with shunt loading structures for impedance matching at low frequencies and small openings for mitigating radiation blockage from the embedded mmWave linear end-fire antenna arrays [100], [116], the sub-6 GHz and mmWave 5G bands can be covered. At the low-frequency communication bands, the radiation is similar to that supported by a conventional cellular handset, while at the mmWave 5G bands, beam steering can be achieved by the end-fire arrays deployed at different places on the handset facets.

3) AIP AND ANTENNA MODULES

Integrated antennas are more attractive than discrete antennas for 5G communications. they can be classified into two categories: antenna-on-chip (AOC) and AIP structures [117]. The AOC integrates antennas with front-end circuitry on the same chip manufactured using mainstream silicon technologies. However, due to the low resistivity and high permittivity associated with silicon substrates, the radiation efficiency of AOC is low [118]. In addition, incorporating an array of antennas in AOC is also challenging because of the limited space on a single chip. The AIP packages an antenna and its array with other integrated radio chips and front-end circuits and makes them into a surface mount chip-scale device. It can overcome the shortcomings of AOC by providing a higher radiation efficiency and a broader bandwidth, while having a high level of integration. Over the past decade, AIP technologies have been widely investigated, including the antenna design, packaging strategies, and interconnection techniques, particularly for 60 GHz wireless systems [119], [120]. Recently, the AIP technologies have been applied to mmWave 5G front-end antenna modules using LTCC stack-ups, high density interconnection (HDI) process based on epoxy/glass RF4, liquid crystal polymers, and embedded wafer level ball grid array (eWLB) [117], [121].

By seamlessly connecting the antennas and RFICs using a multi-layer layout, an integrated antenna module can be devised that improves the overall system performance. As shown in Fig. 16, based on organic multilayer substrates, a

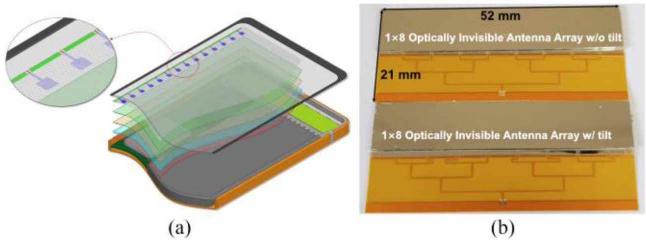

FIGURE 17. **(a) Illustration of AOD for cellular handsets and (b) photographs of optically transparent diamond-grid antenna arrays (reproduced from [129]).**

phased array antenna module with 64 dual-polarized elements was demonstrated by IBM at 28 GHz, achieving a scanning range of $\pm 50^{\circ}$ and throughput of 20.64 Gb/s [122]. Such dual-polarized antenna array modules for massive MIMO working in the *Ka*-band have also been reported by industrial companies, including Nokia Bell Labs [37], Ericsson [123], and NXP Semiconductors [124]. More recently, based on a multi-layer vertical interconnection structure, a vertically-polarized antenna array module was demonstrated where the array was flip-chip mounted on the top layer of the routing board [125].

4) ANTENNA-ON-DISPLAY (AOD)

Due to the trend of increasing the display size of a UT and the strong impact of a human body part (e.g., hand) on antenna performance, deploying antenna arrays in the bezel region of the UTs becomes more and more challenging. Alternatively, embedding the antennas into a display screen, if possible, becomes another viable path, which is referred to as antenna-on-display (AOD) [126]. The advantages of such an integration are that the integrity of the metallic frame is not destroyed since the display area is less exposed to users' hands in the near field.

The first main issue for AOD is the material selection, where optically invisible conductive and insulating materials need to be used. The optical transparency of the stack-up radiating structure of the adopted materials should be higher than 80%, in order for the display to function properly with organic light-emitting diodes or liquid crystal displays. Secondly, the other main challenge is the proper design of the AOD structure and module for achieving beam steering, high efficiency, and wide signal coverage. Over the past decade, various types of transparent antennas, such as patches, dipole, and wide-band monopoles, have been studied since a decade ago using materials including Indium Tin oxide (ITO), silver alloy, polydimethylsiloxane (PDMS), glass, and so on [126]–[128]. More recently, a phased array based on transparent diamond-grid patches made of silver alloy was proposed, demonstrating the possibility of beamforming using AOD located on the rim of the handset display screen [129] (see Fig. 17).

D. mmWAVE ANTENNAS FOR 6G COMMUNICATIONS

For 6G communications, antenna designs face more challenges in the following aspects. First, multi-band operation is needed such that, in the same aperture, multiple services in different mmWave bands as well as the sub-6 GHz bands can be supported. This calls for innovative three-dimensional structural designs and advanced aperture sharing methods. Secondly, reconfigurable mmWave antennas are highly desirable, for switching between different operational bands or pattern modes for versatile applications. Thirdly, the large scale and seamless integration of mmWave chips operating at different bands with the antennas in the same module is required. It involves packaging designs, fabrication process, and heat dissipation consideration.

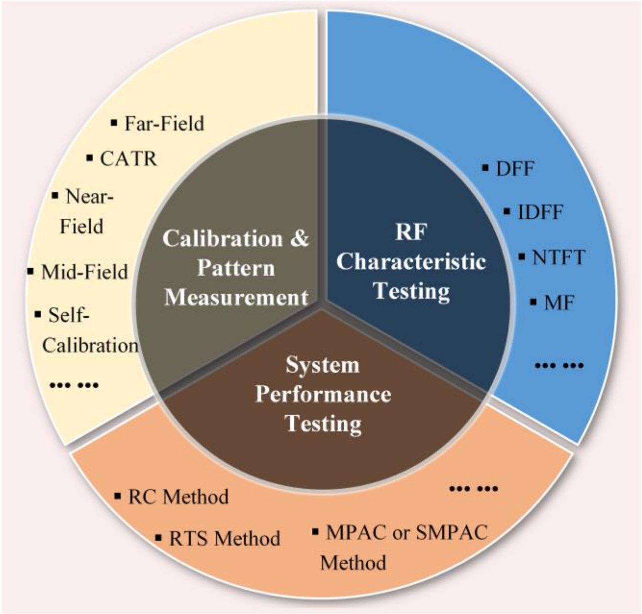

FIGURE 18. **Classification of mmWave measurements and testing.**

V. MEASUREMENT TECHNIQUES FOR 5G/6G ARRAY SYSTEMS

As a large number of RF channels will be used in mmWave 5G BSs, traditional approaches of characterization and measurements would be practically time-consuming. Additionally, the direct-integration of antennas and active components in a mmWave system would leave no ports for direct antenna or RF channel measurements. As a result, over-the-air (OTA) testing has become the mainstream method for system characterization at mmWave frequencies [20], [130], [131].

Based on the procedures, mmWave measurements and testings using the OTA method can be divided into three categories: pattern measurement and calibration, RF characteristic testing, and system performance testing [see Fig. 18]. In this section, a detailed overview of 5G mmWave measurement and testing will be provided. Moreover, challenges and outlooks of 6G testing will also be discussed.

A. PATTERN MEASUREMENT AND CALIBRATION

Beamforming technique has been widely used in mmWave systems for it not only enhances the system capacity but also mitigates the fading effect by increasing the signal-to-noise ratio (SNR) [132]. The accurate pattern measurement requires a proper system calibration, which requires a proper compensation of both amplitudes and phases among all the channels. After the system is calibrated, the beamforming pattern measurement can be performed. Typically, the pattern measurement and calibration methods of a large-scale array can be classified into the far-field method, compact antenna test range (CATR) method, near-field method, and the recently reported mid-field (MF) method.

Traditionally, pattern measurement and calibration are performed in the Fraunhofer zone, where the distance between the probe and device under test (DUT) is larger than $2D^2/\lambda_0$ [133]. Here, D is the largest dimension of the DUT and λ_0 is the free-space wavelength at the carrier frequency. At this distance, the phase variation of the field across the aperture of the DUT is less than 22.5°. The far-field measurement is one of the most commonly used approaches for radiation pattern measurements. The measurement process of large-scale arrays is described in [134], [135]. It shifts the element in an array successively from 0 to 360 degrees and measures the complex electric field formed on the designated observation plane. When the maximum or the minimum power of the array is obtained, the system calibration is finished. The calibration method is an amplitude-only calibration method. This has been successfully implemented in calibrating a *Ka*-band digital beamforming transmitter array [136]. The calibration method is straightforward but time-consuming. Improvements in this conventional calibration have been presented to reduce the measurement time [137], [138]. Similar to the REV calibration method, switching the phase shifter in each channel between 0 and 180 degrees by following a certain order can also achieve system calibration [28], [139], [140]. It makes the measurement faster. The aforementioned methods are usually implemented for analog phased array systems. For full-digital arrays, orthogonal codes like Zadoff-Chu sequence [141], Hadamard matrix [142], and Walsh code [143] can be used in the transmitter array calibration and pattern measurement. It is performed by encoding the transmitting signals of each channel and decoding them on the receiving/observation side, which offers fast system calibration.

Although far-field measurement is direct and efficient, it might face a challenge in measuring mmWave devices for the following reasons. First, millimeter waves suffer from a higher free-space path loss than waves at frequencies below 6 GHz, leading to a lower received signal on the calibration side. The weaker received signal will introduce uncertainties, thus affecting the accuracy of the calibration results. Secondly, mmWave devices and modules are usually physically small, making them more difficult to achieve system alignment in the far-field zone. Based on these facts, the CATR and near-field measurements are more convenient than far-field measurements. The CATR method is based on the geometrical optics theory, which utilizes a paraboloid reflector to convert a spherical wave into a quasi-plane wave inside a quiet zone [144]. It can shrink the chamber's measurement size and has already been adopted in 5G mmWave system measurements [145], [146]. As the signal impinged on the DUT has a quasi-planar wavefront in the quiet zone, the calibration and pattern measurement procedure are similar to that of the aforementioned far-field method. Besides the CATR method, the near-field calibration and pattern measurement method can further minimize the measurement distance. For system calibration, the most commonly used near-field calibration method is the back-propagation method, which is based on the Fourier relationship between the near- and far-zone field quantities [147], [148]. The back-propagation method can also be used as an efficient tool to diagnose defective elements in an active antenna array. Another comprehensive near-field calibration method is the equivalent currents method. It derives the equivalent sources on a Huygens surface that is directly attached to the array aperture [149]. In [150], this method was performed on an array of 1024 waveguide antennas centered at 75 GHz. The above two near-field calibration methods use either planar scanning or spherical scanning to calibrate large-scale antenna systems. An industrial robot can get involved in measuring mmWave probe-fed modules and chips [151], which is compact and lightweight, thereby facilitating chip-level measurements. For pattern measurement using near-field data, the near-field to far-field transformation (NFTF) is utilized, which has been well summarized in [152].

In general, the NFTF uses both the amplitude and phase information at each sampling point on the testing plane. However, acquiring phase information accurately is not easy at mmWave frequencies. On the one hand, phase stability and position precession of the testing system are not guaranteed. On the other hand, for highly integrated up/down-converter systems, measuring the absolute phases from the DUT in the near-field could be difficult. Apart from adding additional hardware circuits [40], near-filed phaseless measurement is also a possible solution [153], [154]. It is based on the idea to reconstruct the phase information from the amplitude-only data by using different phase retrieval approaches [155]–[157].

Recently, MF measurements were proposed for 5G mmWave massive MIMO testing by Keysight Labs [158], [159]. With the MF method, calibration and pattern measurement procedure can be simplified. Because the test system probe antennas are in the far field of the antenna elements, far-field calibration method can be used for system calibration by precisely moving the probe antenna successively [see Fig. 19]. Such a calibration approach has been reported in the literature [40]. For pattern measurement, the far-field array patterns can be derived by multiplying the measured MF patterns with a correction factor (CF). As an example, a *Ka*-band 8×8 element array was calibrated and measured using the MF method, and the pattern measurement results are shown in Fig. 19.

All the above-mentioned calibration methods can be categorized into off-line calibration, where the calibration is carried out in anechoic chambers or laboratories [160], and on-line calibration, also referred to as self-calibration, which is a

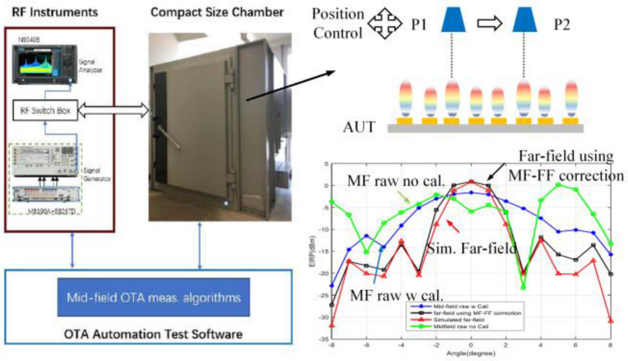

FIGURE 19. **Calibration and pattern measurement using MF method (reproduced from [159]).**

TABLE 3. **OTA RF Metrics for mmWave AAU Conformance Testing**

Tx	Directional Requirement	• Radiated Transmit Power
		• OTA Output Power Dynamic Range
		• OTA Transmit Signal Quality
		• OTA Occupied Bandwidth
	TRP Requirement	• OTA Output Power
		• OTA Transmit OFF Power
		• OTA ACLR
		• OTA Operating Band Unwanted Emission
		• OTA Transmitter Spurious Emission
Rx	Directional Requirement	• OTA Reference Sensitivity Level
		• OTA In-band Selectivity and Blocking
		• OTA Out-of-band Blocking
		• OTA Receiver Intermodulation
		• OTA In Channel Selectivity
	TRP Requirement	• OTA Receiver Spurious Emission

dynamic calibration automatically carried out after the system is deployed. The phase and amplitude variation in mmWave active components as a function of time are reported in [161], indicating the necessity of system self-calibration. In these self-calibration methods, the mutual coupling-based approach [162], [163], toggling the phase shifter of the channel [164], [165], and using a reference antenna through the OTA path can be applied.

B. RF CHARACTERISTIC TESTING

The RF characteristics, such as adjacent channel leakage ratio (ACLR), error vector magnitude (EVM), and harmonic suppression level, have long been adopted as efficient metrics to characterize the performance of RF channels and systems. As mentioned above, these characteristics are usually recorded in OTA measurements for mmWave wireless systems. The typical OTA RF metrics for performance testing of mmWave AAUs are specified by 3GPP [130], which are summarized in Table 3. Also, a few new OTA parameters have been investigated for better describing the performance of the AAU systems. For instance, Leinonen *et al.* demonstrated the use of the EVM-based beamwidth of the radiated beam for characterizing the coverage of the mmWave BSs [166]. A beam EIRP (BEIRP) was proposed to reflect a certain beam radiated transmit power in multibeam mmWave AAU system [167]. Based on the measurement distance, the OTA RF characteristic testing can be classified into the direct far-field (DFF) method, indirect far-filed (IDFF) method, and NTFT based method. They have been documented in 3GPP TR 38. 810 [168].

The direct far-field method has been conducted in a far-field anechoic chamber. As mentioned in sub-Section V.A. It is the most direct and comprehensive testing method. However, it still faces several challenges. On the one hand, the phase curvature of 22.5° in the impinging field might affect the measurement of wideband modulated signals, which could be wider than 400 MHz in the mmWave bands. On the other hand, the measurement distance that satisfies the far-field criterion will become unacceptably large for mmWave arrays using *Blak-Box* approach [169]. In addition, a longer distance will cause more free-space path loss at mmWave frequencies, which would severely degrade the SNR of the received signals.

The indirect far-filed method relies on forming a quasi-plane wave in a short test range, in which the CATR method is one of the indirect far-field methods that have been approved by 3GPP [168]. CATR can transform a spherical wave into a quasi-plane wave in a short range using a reflector, while the quality of the generated testing zone, i.e., the quiet zone, is dependent on the performance of the reflector. The size of the quiet zone is usually half of the size of the reflector [170]. Although CATR is promising for mmWave and even sub-THz measurements, the cost is high due to the employed reflector.

The NFTF method can also shorten the test range and has been a mature approach in array calibration and pattern measurement. However, there still exist some unsolved issues. For example, the relationship between the modulated signals measured in the near-field and far-field regions needs to be theoretically and experimentally investigated and verified.

Apart from the above three methods suggested by 3GPP, other methods have also been proposed. The plane wave converter (PWC) method is another IDF method, which uses an active antenna array to form a quasi-plane wave in a short testing range by adjusting the phase and amplitude of each channel of the PWC array [171]. Unlike the CATR method, this method utilizes active components inside the passive reflector and achieves an adjustable quiet zone within a reduced space compared with the CATR method [172]. However, the PWC method has only been applied to a narrow bandwidth. The wideband implementation needs to be further studied. Another method is the MF method as mentioned in sub-Section V.A. Instead of the complex NFTF, some of the RF performance parameters are obtained by multiplying the MF measurement results with a correction factor. The MF method supports the testing of all the RF performance parameters listed in Table 3, which has been demonstrated and proved in detail in [159]. However, the efficiency and accuracy of both the PWC and MF methods need to be further verified in the mmWave bands.

C. SYSTEM PERFORMANCE TESTING

The system performance testing includes system throughput, beam management, and link performance of the UE testing, *etc.* It is a systematic evaluation of the DUT in a wireless environment. Outdoor field testing is direct and accurate but faces challenges of uncontrollable and unrepeatable channel parameters. Hence, a channel emulator plays an important role in system performance testing, which is used to reconstruct the actual channel environment in the laboratory. It is currently being developed towards a larger bandwidth, a higher frequency, and increased channel number for 5G mmWave communications [173]. The system performance testing methods, with the help of the channel emulators, include the reverberation chamber (RC) method, radiated two steps (RTS) method, and multi-probe anechoic chamber (MPAC) method.

A RC is made of a metallic stirrer to excite electromagnetic modes inside a metal-shielded cavity, such that the rich multipath Rayleigh channels can be constructed [174]. As electromagnetic modes are quasi-equally distributed in the cavity, the RC method has often been used for testing the MIMO capacity of the UE [175] and the absorption of a phantom [176]. Nevertheless, for highly sparse mmWave channels in the BSs, the RC method needs to be improved [177].

The RTS method [178] has been approved as a MIMO OTA test method by 3GPP [179], which is based on the idea of separating the system performance testing into the antenna array pattern measurement in the anechoic chamber and the system performance testing using cables in the laboratory. After acquiring the complex pattern information of the array, the pattern information, the transfer matrix linking the DUT ports and the antenna array ports, and the channel information can all be generated in the channel emulator. The former step is performed by measuring at the antenna array ports, while the latter step is carried out by measuring at the DUT ports through cables. The RTS method has been used in system performance testing at frequencies below 6 GHz [180], [181]. However, because the antennas and DUTs need to be separated in this method, its application is limited in testing highly integrated mmWave terminals. Moreover, the effect of the antenna is ignored for system performance evaluation.

The MPAC method was standardized by the Cellular Telecommunications Industry Association (CTIA) to test the LTE downlink MIMO OTA performance in the early years [182]. It is one of the mainstream methods for testing the system performance of 5G mmWave devices. Traditionally, the MPAC uses several probe antennas enclosing the DUT in a ring. Each probe is connected to an emulator channel to construct the targeted multipath environment [183]. The emulation accuracy in the testing area depends on the number of probes and their positions. For sparse mmWave channels, a cost-effective sectored MPAC was proposed in [184], [185], which uses mmWave switching circuits to select the probes with the strongest effect and map them to the mmWave channel emulators [see Fig. 20] [186]. It can be used to test the mmWave massive MIMO systems and UEs for both the line-of-sight (LOS) and non-line-of-sight (NLOS) links. Nevertheless, the system cost and complexity of the MPAC and sectored MPAC methods are higher than the RC and RTS methods. In recent years, probe selection algorithms are under investigation to further reduce the number of active probes.

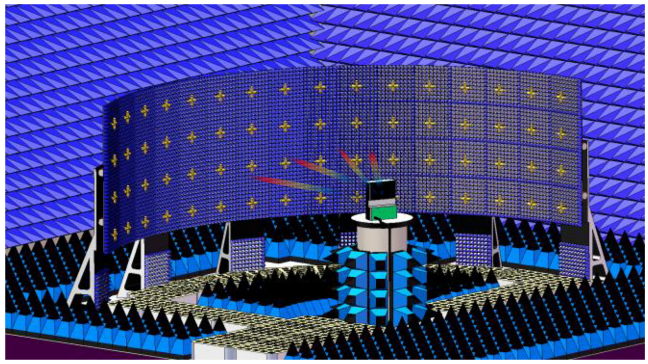

FIGURE 20. **The conceptual setup of the sectored MPAC testing system [186].**

D. OUTLOOKS OF TESTING METHODS FOR 6G COMMUNICATIONS

Overall, the unlicensed bandwidth is relatively abundant in mmWave band, but the free-space path loss becomes far greater than that of the sub-6 GHz band. They force the testing techniques to move to higher frequencies, broader bandwidth, and larger dynamic ranges. For the 6G communications, new potential technologies will raise new challenges in OTA measurements. First, for asymmetrical wireless systems mentioned in Section II, the end-to-end system performance testing is required because the channel matrices for the downlink and uplink communications are different. This end-to-end measurement conception has already been reported in [187] for 5G performance testing and could be utilized fort testing asymmetrical wireless systems. Secondly, terminal mobility is characterized as the Doppler shift included in the state-of-art system performance testing, but it needs to be greatly improved for testing mmWave satellite communications. The dynamic target detection, doppler shift of moving directions, and link stability should all be considered in system performance testing in an anechoic chamber, as it is nearly impossible to do in-situ test by launching a satellite.

VI. CHANNEL CHARACTERIZATION

As frequency increases, the channel characteristics in mmWave bands are significantly different from those in the sub-6 GHz bands in terms of large-scale and small-scale fading [188]. Real-world channel sounding results reveal that mmWave signals are more vulnerable to surrounding blockages. Also, the sparsity nature of the channel is discernible, which poses several challenges for exploiting the advantages of mmWave communications [189], [190]. Moreover, when large-scale antenna arrays confined within a limited physical space are used at BSs, they are expected to provide sufficient directional beamforming gains to combat severe path loss at mmWave frequencies. An increasing number of elements, however, presents several new challenges to be addressed, such as channel hardening, spherical wave propagation, and spatial non-stationarity [191]. Therefore, the interaction between antennas and propagation channel needs to be investigated in order to meet the requirements of future mmWave massive MIMO systems.

For mmWave communications, the path losses are generally much higher especially in NLOS scenarios [189], [190]. Additional losses including shadow fading, blockage effect, foliage attenuation, and off-body fading (e.g., handset on the right side of the head) need to be taken into account [192], [193]. The statistical analysis of these effects can be performed via site-specific measurements rather than conducting cellular-type measurements. Another issue is that most work so far mainly focuses on omnidirectional path loss characterization. The effects of beam patterns and antenna polarization in different transmission schemes still remain unclear.

The small-scale space-time propagation characteristics play a critical role in mmWave system designs, including the antennas, RF front-ends, access protocols, and network architectures [188], [193]. Apart from the LOS path, multipath propagation occurs that combines the reflected and diffracted paths. Thus, it is meaningful to study the reflection and diffraction over various materials in different frequency bands and at different incident angles. Owing to channel bandwidth increase, relatively high delay resolution results in multipath effects observable in mmWave sparse channels. Thus, the delay spread and power decay for each cluster propagating through a physical or virtual scatterer need to be estimated. The high spatial resolution of large-scale antenna arrays can leverage the benefits of 3D beamforming in both the azimuthal and elevation planes. They will enable higher multi-user capacity, coverage enhancement, and suppression of multi-cell and inter-beam interference. A major issue of exploiting the channel's elevation degree of freedom is that the power consumption will increase as the elevation angle increases. Consequently, a full description of the three polarizations of mmWave channels in a uniform Cartesian coordinate system is necessary. The recent development of mmWave channel measurement techniques using virtual antenna arrays reveal that the spaced elements will observe different sets of clusters (so-called spatial non-stationarity property), which can be modeled as a birth-death process [191]. Overall, with the knowledge of propagation characteristics and their interactions with the RF subsystems, the rapid development of the mmWave technologies could unlock the full potential of the mmWave spectrum in the future 5G/6G wireless communication systems.

VII. CONCLUSION

In summary, the key enabling mmWave technologies for 5G communications are reviewed, including the different kinds of system architectures, multi-channel beamforming chips, antennas for BSs and UTs, measurement and calibration techniques, and wireless channel characterization. The recent developments are described with examples, and the requirements and challenges for 6G communications are also discussed. In general, compared with 5G, the 6G requires the integration of more physical transceiver channels, more frequency bands, more operation flexibility, and more diverse functionalities into a communication system with considerably superior electrical performance. This calls for the development of low-power highly-linear multi-channel chips, multi-band multi-polarization compact antennas and modules, automated efficient calibration and measurement methods, multi-dimensional beamforming networks, accurate multi-spectral multi-stage channel models, and many other enabling mmWave hardwares and related algorithms. It is believed that the mmWave technology will play a more and more important role than it ever has been in future commercial telecommunication infrastructures.

REFERENCES

[1] G. Falciasecca, "Marconi's early experiments in wireless telegraphy, 1895," *IEEE Antennas Propag. Mag.*, vol. 52, no. 6, pp. 220–221, Dec. 2010.

[2] T. S. Rappaport, *Wireless Communications: Principles and Practice*, 2nd ed. Englewood Cliffs, NJ, USA: Prentice-Hall, 2002.

[3] A. Goldsmith, *Wireless Communications*. Cambridge, U.K.: Cambridge Univ., 2005.

[4] J. A. del Peral-Rosado, R. Raulefs, J. A. López-Salcedo, and G. Seco-Granados, "Survey of cellular mobile radio localization methods: From 1G to 5G," *IEEE Commun. Surveys Tuts.*, vol. 20, no. 2, pp. 1124–1148, 2nd Quart. 2018.

[5] T. Farley, "Mobile telephone history," *Telektronikk*, vol. 101, no. 3–4, pp. 22–34, 2005.

[6] *GSM Memorandum of Understanding*, Copenhagen, Denmark, Eur. CEPT, Sep. 1987.

[7] F. Hillebrand, "The creation of standards for global mobile communication: GSM and UMTS standardization from 1982 to 2000," *IEEE Wireless Commun.*, vol. 20, no. 5, pp. 24–33, Oct. 2013.

[8] H. Holma and A. Toskala, *WCDMA For UMTS: Radio Access For Third Generation Mobile Communications*. Chichester, U.K.: Wiley, 2000.

[9] S. Abeta, M. Tanno, and M. Iwamura, "Standardization trends in LTE enhancement," *NTT DOCOMO Tech. J.*, vol. 12, no. 1, pp. 42–44, Jun. 2010.

[10] C. Hoymann *et al.*, "LTE release 14 outlook," *IEEE Wireless Commun.*, vol. 54, no. 6, pp. 44–49, Jun. 2016.

[11] S. Chen and J. Zhao, "The requirements, challenges, and technologies for 5G of terrestrial mobile telecommunication," *IEEE Commun. Mag.*, vol. 52, no. 5, pp. 36–43, May 2014.

[12] J. G. Andrews *et al.*, "Overview of millimeter wave communications for fifth-generation (5G) wireless networks—With a focus on propagation models," *IEEE J. Sel. Areas Commun.*, vol. 32, no. 6, pp. 1065–1082, Jun. 2014.

[13] W. Saad, M. Bennis, and M. Chen, "A vision of 6G wireless systems: Applications, trends, technologies, and open research problems," *IEEE Netw.*, vol. 34, no. 3, pp. 134–142, May 2020.

[14] A. Osseiran *et al.*, "Scenarios for 5G mobile and wireless communications: The vision of the METIS project," *IEEE Commun. Mag.*, vol. 52, no. 5, pp. 26–35, May 2014.

[15] E. Dahlman *et al.*, "5G wireless access: Requirements and realization," *IEEE Commun. Mag.*, vol. 52, no. 12, pp. 42–47, Dec. 2014.

[16] F. Boccardi, R. W. Heath, Jr., A. Lozano, T. L. Marzetta, and P. Popovski, "Five disruptive technology directions for 5G," *IEEE Commun. Mag.*, vol. 52, no. 2, pp. 74–80, Feb. 2014.

[17] C.-X. Wang *et al.*, "Cellular architecture and key technologies for 5G wireless communication networks," *IEEE Commun. Mag.*, vol. 52, no. 2, pp. 122–130, Feb. 2014.
[18] T. S. Rappaport *et al.*, "Millimeter wave mobile communications for 5G cellular: It will work!," *IEEE Access*, vol. 1, pp. 335–349, May 2013.
[19] J. Qiao, X. Shen, J. Mark, Q. Shen, Y. He, and L. Lei, "Enabling deviceto-device communications in millimeter-wave 5G cellular networks," *IEEE Commun. Mag.*, vol. 53, no. 1, pp. 209–215, Jan. 2015.
[20] NR; Base Station (BS) Radio Transmission and Reception (Release 16), document 3GPP TS 38.104, 2019.
[21] J. Lee *et al.*, "Spectrum for 5G: Global status, challenges, and enabling technologies," *IEEE Commun. Mag.*, vol. 56, no. 3, pp. 12–18, Mar. 2018.
[22] W. Hong *et al.*, "Multibeam antenna technologies for 5G wireless communications," *IEEE Trans. Antennas Propag.*, vol. 65, no. 12, pp. 6231–6249, Dec. 2017.
[23] J. Kibilda *et al.*, "Indoor millimeter-wave systems: Design and performance evaluation," *Proc. IEEE*, vol. 108, no. 6, pp. 923–944, Jun. 2020.
[24] Y. Wang *et al.*, "A 39-GHz 64-element phased-array transceiver with built-in phase and amplitude calibrations for large-array 5G NR in 65-nm CMOS," *IEEE J. Solid-State Circuits*, vol. 55, no. 5, pp. 1249–1269, May 2020.
[25] T. S. Rappaport, Y. Xing, G. R. MacCartney, A. F. Molisch, E. Mellios, and J. Zhang, "Overview of millimeter wave communications for fifth-generation (5G) wireless networks—With a focus on propagation models," *IEEE Trans. Antennas Propag.*, vol. 65, no. 12, pp. 6213–6230, Dec. 2017.
[26] H. Viswanathan and P. E. Mogensen, "Communications in the 6G era," *IEEE Access*, vol. 8, pp. 57063–57074, Mar. 2020.
[27] T. S. Rappaport *et al.*, "Wireless communications and applications above 100 GHz: Opportunities and challenges for 6G and beyond," *IEEE Access*, vol. 7, pp. 78729–78757, Mar. 2019.
[28] B. Yang, Z. Yu, R. Zhang, J. Zhou, and W. Hong, "Local oscillator phase shifting and harmonic mixing-based high-precision phased array for 5G millimeter-wave communications," *IEEE Trans. Microw. Theory Techn.*, vol. 67, no. 7, pp. 3162–3173, Jul. 2019.
[29] R. Zhang, J. Zhou, J. Lan, B. Yang, and Z. Yu, "A high-precision hybrid analog and digital beamforming transceiver system for 5G millimeter-wave communication," *IEEE Access*, vol. 7, pp. 83012–83023, Jun. 2019.
[30] M. Jiang, Z. N. Chen, Y. Zhang, W. Hong, and X. Xuan, "Metamaterial based thin planar lens antenna for spatial beamforming and multibeam massive MIMO," *IEEE Trans. Antennas Propag.*, vol. 65, no. 2, pp. 464–472, Feb. 2017.
[31] S.-S. Jeon, Y. Wang, Y. Qian, and T. Itoh, "A novel smart antenna system implementation for broad-band wireless communications," *IEEE Trans. Antennas Propag.*, vol. 50, no. 5, pp. 600–606, May 2002.
[32] D. Kang, K. Koh, and G. M. Rebeiz, "A Ku-band two-antenna four-simultaneous beams sige BiCMOS phased array receiver," *IEEE Trans. Microw. Theory Techn.*, vol. 58, no. 4, pp. 771–780, Apr. 2010.
[33] M. Sayginer and G. M. Rebeiz, "An eight-element 2–16-GHz programmable phased array receiver with one two or four simultaneous beams in sige BiCMOS," *IEEE Trans. Microw. Theory Techn.*, vol. 64, no. 12, pp. 4585–4597, Dec. 2016.
[34] K. Tekkouk, J. Hirokawa, R. Sauleau, M. Ettorre, M. Sano, and M. Ando, "Dual-layer ridged waveguide slot array fed by a butler matrix with sidelobe control in the 60-GHz band," *IEEE Trans. Antennas Propag.*, vol. 63, no. 9, pp. 3857–3867, Sep. 2015.
[35] P. Chen, W. Hong, Z. Kuai, and J. Xu, "A double layer substrate integrated waveguide blass matrix for beamforming applications," *IEEE Microw. Wireless Compon. Lett.*, vol. 19, no. 6, pp. 374–376, Jun. 2009.
[36] Y. Zeng, R. Zhang, and Z. N. Chen, "Electromagnetic lens-focusing antenna enabled massive MIMO: Performance improvement and cost reduction," *IEEE J. Sel. Areas Commun.*, vol. 32, no. 6, pp. 1194–1206, Jun. 2014.
[37] R. Valkonen, "Compact 28-GHz phased array antenna for 5G access," in *IEEE MTT-S Int. Microw. Symp. Dig.*, Philadelphia, PA, USA, Jun. 2018, pp. 1334–1337.
[38] B. Yang, Z. Yu, J. Lan, R. Zhang, J. Zhou, and W. Hong, "Digital beamforming-based massive MIMO transceiver for 5G millimeter-wave communications," *IEEE Trans. Microw. Theory Techn.*, vol. 66, no. 7, pp. 3403–3418, May 2018.
[39] C. Yu *et al.*, "Full-angle digital predistortion of 5G millimeter-wave massive MIMO transmitters," *IEEE Trans. Microw. Theory Techn.*, vol. 67, no. 7, pp. 2847–2860, Jul. 2019.
[40] L. Kuai *et al.*, "A N260 band 64 channel millimeter wave full-digital multi-beam array for 5G massive MIMO applications," *IEEE Access*, vol. 8, pp. 47640–47653, Mar. 2020.
[41] M. M. Molu, P. Xiao, M. Khalily, K. Cumanan, L. Zhang, and R. Tafazolli, "Low-complexity and robust hybrid beamforming design for multi-antenna communication systems," *IEEE Trans. Wireless Commun.*, vol. 17, no. 3, pp. 1445–1459, Dec. 2018.
[42] J. A. Zhang, X. Huang, V. Dyadyuk, and Y. J. Guo, "Massive hybrid antenna array for millimeter-wave cellular communications," *IEEE Wireless Commun*, vol. 22, no. 1, pp. 79–87, Feb. 2015.
[43] X. Liu *et al.*, "Beam-oriented digital predistortion for 5G massive MIMO hybrid beamforming transmitters," *IEEE Trans. Microw. Theory Techn.*, vol. 66, no. 7, pp. 3419–3432, Jul. 2018.
[44] S. Payami *et al.*, "Developing the first MMWave fully-connected hybrid beamformer with a large antenna array," *IEEE Access*, vol. 8, pp. 141282–114129, Jul. 2020.
[45] Y. Gao, M. Khaliel, F. Zheng, and T. Kaiser, "Rotman lens based hybrid analog–digital beamforming in massive MIMO systems: Array architectures, beam selection algorithms and experiments," *IEEE Trans. Veh. Technol.*, vol. 66, no. 10, pp. 9134–9148, Jun. 2017.
[46] Y. Hu and W. Hong, "A novel hybrid analog-digital multibeam antenna array for massive MIMO applications," in *Proc. IEEE Asia-Pacific Conf. Antennas Propag.,* Auckland, New Zealand, Aug. 2018, pp. 42–45.
[47] J. D. Dunworth *et al.*, "A 28 GHz bulk-CMOS dual-polarization phased-array transceiver with 24 channels for 5G user and base station equipment," in *Proc. IEEE Int. Solid-State Circuits Conf.*, San Francisco, CA, USA, Feb. 2018, pp. 70–72.
[48] W. He, B. Xu, Y. Yao, D. Colombi, Z. Ying, and S. He, "Implications of incident power density limits on power and EIRP levels of 5G millimeter-wave user equipment," *IEEE Access*, vol. 8, pp. 148214–148225, Aug. 2020.
[49] D. Liu, X. Gu, C. W. Baks, and A. Valdes-Garcia, "Antenna-in-package design considerations for Ka-band 5G communication applications," *IEEE Trans. Antennas Propag.*, vol. 65, no. 12, pp. 6372–6379, Dec. 2017.
[50] T. Kuwabara, N. Tawa, Y. Tone, and T. Kaneko, "A 28 GHz 480 elements digital AAS using GaN HEMT amplifiers with 68 dBm EIRP for 5G long-range base station applications," in *Proc. IEEE Compound Semicond. Integr. Circuit Symp.*, Oct. 2017, pp. 1–4.
[51] J. Park, S. Y. Lee, Y. Kim, J. Lee, and W. Hong, "Hybrid antenna module concept for 28 GHz 5G beamsteering cellular devices," in *Proc. IEEE MTT-S Int. Microw. Workshop Ser. 5G Hardware Syst. Technol.*, Dublin, Ireland, pp. 1–3, Aug. 2018.
[52] C. I. Q. Sun, Z. Liu, S. Zhang, and S. Han, "The big-data-driven intelligent wireless network: Architecture, use cases, solutions, and future trends," *IEEE Veh. Technol. Mag.*, vol. 12, no. 4, pp. 20–29, Dec. 2017.
[53] J. Liu, Y. Shi, Z. M. Fadlullah, and N. Kato, "Space-air-ground integrated network: A survey," *IEEE Commun. Surveys Tuts.*, vol. 20, no. 4, pp. 2714–2741, Fourth quarter 2018.
[54] J. Foust, "SpaceX's space-Internet woes: Despite technical glitches, the company plans to launch the first of nearly 12,000 satellites in 2019," *IEEE Spectr.*, vol. 56, no. 1, pp. 50–51, Jan. 2019.
[55] I. del Portillo Barrios, B. Cameron, and E. Crawley, "A technical comparison of three low earth orbit satellite constellation systems to provide global broadband," *Acta Astronautica*, vol. 159, 2019.
[56] C. G. Christodoulou, Y. Tawk, S. A. Lane, and S. R. Erwin, "Reconfigurable antennas for wireless and space applications," *Proc. IEEE*, vol. 100, no. 7, pp. 2250–2261, Jul. 2012.
[57] K. B. Letaief, W. Chen, Y. Shi, J. Zhang, and Y. A. Zhang, "The roadmap to 6G: AI empowered wireless networks," *IEEE Commun. Mag.*, vol. 57, no. 8, pp. 84–90, Aug. 2019.

[58] C. Wang, M. D. Renzo, S. Stanczak, S. Wang, and E. G. Larsson, "Artificial intelligence enabled wireless networking for 5G and beyond: Recent advances and future challenges," *IEEE Wireless Commun.*, vol. 27, no. 1, pp. 16–23, Feb. 2020.
[59] J. Riihijarvi and P. Mahonen, "Machine learning for performance prediction in mobile cellular networks," *IEEE Comput. Intell. Mag.*, vol. 13, no. 1, pp. 51–60, Feb. 2018.
[60] C. Guo *et al.*, "Design and implementation of a full-digital beamforming array with nonreciprocal tx/rx beam patterns," *IEEE Antennas Wireless Propag. Lett.*, vol. 19, no. 11, pp. 1978–1982, Nov. 2020.
[61] K. Kibaroglu, M. Sayginer, T. Phelps, and G. M. Rebeiz, "A 64-element 28-GHz phased-array transceiver with 52-dBm EIRP and 8–12-Gb/s 5G link at 300 meters without any calibration," *IEEE Trans. Microw. Theory Techn.*, vol. 66, no. 12, pp. 5796–5811, Dec. 2018.
[62] K. Kibaroglu, M. Sayginer, and G. M. Rebeiz, "A low-cost scalable 32-element 28-GHz phased array transceiver for 5G communication links based on a 2 × 2 beamformer flip-chip unit cell," *IEEE J. Solid-State Circuits*, vol. 53, no. 5, pp. 1260–1274, May 2018.
[63] B. Sadhu *et al.*, "A 28-GHz 32-element TRX phased-array IC with concurrent dual-polarized operation and orthogonal phase and gain control for 5G communications," *IEEE J. Solid-State Circuits*, vol. 52, no. 12, pp. 3373–3391, Dec. 2017.
[64] J. Pang *et al.*, "A 28-GHz CMOS phased-array transceiver based on LO phase-shifting architecture with gain invariant phase tuning for 5G new radio," *IEEE J. Solid-State Circuits*, vol. 54, no. 5, pp. 1228–1242, May 2019.
[65] C. A. Balanis, *Antenna Theory: Analysis and Design*, 4th ed. Hoboken, NY, USA: Wiley, 2016.
[66] W. Hong, K.-H. Baek, and S. Ko, "Millimeter-wave 5G antennas for smartphones: Overview and experimental demonstration," *IEEE Trans. Antennas Propag.*, vol. 65, no. 12, pp. 6250–6261, Dec. 2017.
[67] T. E. Bogale and L. B. Le, "Massive MIMO and MMWave for 5G wireless hetnet: Potential benefits and challenges," *IEEE Veh. Technol. Mag.*, vol. 11, no. 1, pp. 64–75, Mar. 2016.
[68] Z. N. Chen and K.-M. Luk, *Antenna For Base Stations in Wireless Communications*. New York, NY, USA: McGraw-Hill, 2009.
[69] G. M. Rebeiz, "Millimeter-wave and terahertz integrated circuit antennas," *Proc. IEEE*, vol. 80, no. 11, pp. 1748–1770, Nov. 1992.
[70] B. Yang, Z. Yu, Y. Dong, J. Zhou, and W. Hong, "Compact tapered slot antenna array for 5G millimeter-wave massive MIMO systems," *IEEE Trans. Antennas Propag.*, vol. 65, no. 12, pp. 6721–6727, Dec. 2017.
[71] K.-M. Mak, K. K. So, H.-W. Lai, and K.-M. Luk, "A magnetoelectric dipole leaky-wave antenna for millimeter-wave application," *IEEE Trans. Antennas Propag.*, vol. 65, no. 12, pp. 6395–6402, Dec. 2017.
[72] Y. Zhu, R. Lu, C. Yu, and W. Hong, "Design and implementation of a wideband antenna subarray for phased array applications," *IEEE Trans. Antennas Propag.*, vol. 68, no. 8, pp. 6059–6068, Dec. 2020.
[73] T. Li and Z. N. Chen, "Wideband sidelobe-level reduced Ka-band metasurface antenna array fed by substrate-integrated gap waveguide using characteristic mode analysis," *IEEE Trans. Antennas Propag.*, vol. 68, no. 3, pp. 1356–1365, Mar. 2020.
[74] D. J. Bisharat, S. Liao, and Q. Xue, "High gain and low cost differentially fed circularly polarized planar aperture antenna for broadband millimeter-wave applications," *IEEE Trans. Antennas Propag.*, vol. 64, no. 1, pp. 33–42, Jan. 2016.
[75] K. Schneider, S. Marahrens, J. Eisenbeis, J. Kowalewski, and T. Zwick, "Broadband dual-polarized stacked microstrip antenna with pin- and edge-feed for 5G applications in Ka-band," in *Proc. 14th Eur. Conf. Antennas Propag.*, Copenhagen, Denmark, Mar. 2020, pp. 1–5.
[76] Q. Yang *et al.*, "Millimetre-wave dual-polarized differentially-fed 2D multibeam patch antenna array," *IEEE Trans. Antennas Propag.*, 2020, early access, doi: 10.1109/TAP.2020.2992896.
[77] H. Chu and Y. Guo, "A filtering dual-polarized antenna subarray targeting for base stations in millimeter-wave 5G wireless communications," *IEEE Trans. Compon. Packag. Manuf. Technol.*, vol. 7, no. 6, pp. 964–973, Jun. 2017.
[78] Y. Li and K.-M. Luk, "60-GHz dual-polarized two-dimensional switch beam wideband antenna array of aperture-coupled magneto-electric dipoles," *IEEE Trans. Antennas Propag.*, vol. 64, no. 2, pp. 554–563, Feb. 2016.
[79] S. J. Yang, Y. M. Pan, L.-Y. Shi, and X. Y. Zhang, "Millimeter-wave dual-polarized filtering antenna for 5G application," *IEEE Trans. Antennas Propag.*, vol. 68, no. 7, pp. 5114–5121, Jul. 2020.
[80] T. Li and Z. N. Chen, "A dual-band metasurface antenna using characteristic mode analysis," *IEEE Trans. Antennas Propag.*, vol. 66, no. 10, pp. 5620–5624, Oct. 2018.
[81] Q. Wu, J. Hirokawa, J. Yin, C. Yu, H. Wang, and W. Hong, "Millimeter-wave multibeam endfire dual-circularly polarized antenna array for 5G wireless applications," *IEEE Trans. Antennas Propag.*, vol. 66, no. 9, pp. 4930–4935, Sep. 2018.
[82] W. M. Dyab, A. A. Sakr, and K. Wu, "Dually-polarized butler matrix for base stations with polarization diversity," *IEEE Trans. Microw. Theory Techn.*, vol. 66, no. 12, pp. 5543–5553, Dec. 2018.
[83] H.-T. Chou, S.-J. Chou, C.-W. Chiu, C.-C. Sun, and C.-T. Yu, "Quasi-orthogonal multibeam radiation of reflector antennas for radio coverage of mobile communication at millimeter-wave frequencies," *IEEE Trans. Antennas Propag.*, vol. 66, no. 11, pp. 6340–6345, Nov. 2018.
[84] Z. H. Jiang, Y. Zhang, J. Xu, Y. Yu, and W. Hong, "Integrated broadband circularly polarized multibeam antennas using Berry-phase transmit-arrays for Ka-band applications," *IEEE Trans. Antennas Propag.*, vol. 68, no. 2, pp. 859–872, Feb. 2020.
[85] Z. Ying, "Antennas in cellular phones for mobile communications," *Proc. IEEE*, vol. 100, no. 7, pp. 2286–2296, Jul. 2012.
[86] W. Hong, "Solving the 5G mobile antenna puzzle: Assessing future directions for the 5G mobile antenna paradigm shift," *IEEE Microw. Mag.*, vol. 18, no. 7, pp. 86–102, Dec. 2017.
[87] General Aspects for User Equipment (UE) Radio Frequency (RF) for NR (Release 15), document 38.817-1, 3GPP, 2019.
[88] J. Helander, K. Zhao, Z. Ying, and D. Sjöberg, "Performance analysis of millimeter-wave phased array antennas in cellular handsets," *IEEE Antennas Wireless Propag. Lett.*, vol. 15, pp. 504–507, 2016.
[89] R. Khan, A. A. Al-Hadi, P. J. Soh, M. R. Kamarudin, M. T. Ali, and Owais, "User influence on mobile terminal antennas: A review of challenges and potential solution for 5G antennas," *IEEE Access*, vol. 6, pp. 77695–77715, Nov. 2018.
[90] S. Shinjo, K. Nakatani, K. Tsutsumi, and H. Nakamizo, "Integrating the front end: A highly integrated RF front end for high-SHF wideband massive MIMO in 5G," *IEEE Microw. Mag.*, vol. 18, no. 5, pp. 31–40, Aug. 2017.
[91] W. Hong, K.-H. Baek, Y. Lee, Y. Kim, and S.-T. Ko, "Study and prototyping of practically large-scale MMWave antenna systems for 5G cellular devices," *IEEE Commun. Mag.*, vol. 52, no. 9, pp. 63–69, Sep. 2014.
[92] R. Suga, H. Nakano, Y. Hirachi, J. Hirokawa, and M. Ando, "Cost-effective 60-GHz antenna package with end-fire radiation for wireless file-transfer system," *IEEE Trans. Microw. Theory Techn.*, vol. 58, no. 12, pp. 3989–3995, Dec. 2010.
[93] S. Zhang, I. Syrytsin, and G. F. Pedersen, "Compact beam-steerable antenna array with two passive parasitic elements for 5G mobile terminals at 28 GHz," *IEEE Trans. Antennas Propag.*, vol. 66, no. 10, pp. 5193–5203, Oct. 2018.
[94] J. Zeng and K. Luk, "Wideband millimeter-wave end-fire magneto-electric dipole antenna with microstrip-line feed," *IEEE Trans. Antennas Propag.*, vol. 68, no. 4, pp. 2658–2665, Apr. 2020.
[95] B. Yu, K. Yang, C.-Y.-D. Sim, and G. Yang, "A novel 28 GHz beam steering array for 5G mobile device with metallic casing application," *IEEE Trans. Antennas Propag.*, vol. 66, no. 1, pp. 462–466, Jan. 2018.
[96] J. Choi *et al.*, "Frequency-adjustable planar folded slot antenna using fully integrated multithrow function for 5G mobile devices at millimeter-wave spectrum," *IEEE Trans. Microw. Theory Techn.*, vol. 68, no. 5, pp. 1872–1881, May 2020.
[97] C. Di Paola, S. Zhang, K. Zhao, Z. Ying, T. Bolin, and G. F. Pedersen, "Wideband beam-switchable 28 GHz quasi-Yagi array for mobile devices," *IEEE Trans. Antennas Propag.*, vol. 67, no. 11, pp. 6870–6882, Nov. 2018.
[98] I. Syrytsin, S. Zhang, G. F. Pedersen, and A. S. Morris, III, "Compact quad-mode planar phased array with wideband for 5G mobile terminals," *IEEE Trans. Antennas Propag.*, vol. 66, no. 9, pp. 4648–4657, Sep. 2018.
[99] S. Zhang, X. Chen, I. Syrytsin, and G. F. Pedersen, "A planar switchable 3-D-coverage phased array antenna and its user effects for 28-GHz mobile terminal applications," *IEEE Trans. Antennas Propag.*, vol. 65, no. 12, pp. 6413–6421, Dec. 2017.

[100] R. Rodriguez-Cano, S. Zhang, K. Zhao, and G. F. Pedersen, "mm-Wave beam-steerable endfire array embedded in a slotted metal-frame LTE antenna," *IEEE Trans. Antennas Propag.*, vol. 68, no. 5, pp. 3685–3694, May 2020.

[101] Y.-W. Hsu, T.-C. Huang, H.-S. Lin, and Y.-C. Lin, "Dual-polarized quasi Yagi-Uda antennas with endfire radiation for millimeter-wave MIMO terminals," *IEEE Trans. Antennas Propag.*, vol. 65, no. 12, pp. 6282–6289, Dec. 2017.

[102] O. Jo, J.-J. Kim, J. Yoon, D. Choi, and W. Hong, "Exploitation of dual-polarization diversity for 5G millimeter-wave MIMO beam-forming systems," *IEEE Trans. Antennas Propag.*, vol. 65, no. 12, pp. 6646–6655, Dec. 2017.

[103] A. Li, K.-M. Lu, and Y. Li, "A dual linearly polarized end-fire antenna array for the 5G applications," *IEEE Access*, vol. 6, pp. 78276–78285, Dec. 2018.

[104] J. Zhang, K. Zhao, L. Wang, S. Zhang, and G. F. Pedersen, "Dual-polarized phased array with end-fire radiation for 5G handset applications," *IEEE Trans. Antennas Propag.*, vol. 68, no. 4, pp. 3277–3282, Apr. 2020.

[105] R. M. Moreno *et al.*, "Dual-polarized mm-Wave end-fire chain-slot antenna for mobile devices," *IEEE Trans. Antennas Propag.*, early access, 2020.

[106] R. Khan, A. A. Al-Hadi, and P. J. Soh, "Recent advancements in user effect mitigation for mobile terminal antennas: A review," *IEEE Trans. Electromagn. Compat.*, vol. 61, no. 1, pp. 279–287, Feb. 2019.

[107] I. Syrytsin, S. Zhang, G. F. Pedersen, K. Zhao, T. Bolin, and Z. Ying, "Statistical investigation of the user effects on mobile terminal antennas for 5G applications," *IEEE Trans. Antennas Propag.*, vol. 65, no. 12, pp. 6596–6605, Dec. 2017.

[108] G. Q. Luo *et al.*, "Filtenna consisting of horn antenna and substrate integrated waveguide cavity FSS," *IEEE Trans. Antennas Propag.*, vol. 55, no. 1, pp. 92–98, Jan. 2007.

[109] Y. Yusuf and X. Gong, "Compact low-loss integration of high-Q 3-D filters with highly efficient antennas," *IEEE Trans. Microw. Theory Technol.*, vol. 59, no. 4, pp. 857–865, Apr. 2011.

[110] Z. H. Jiang and D. H. Werner, "A compact, wideband circularly polarized co-designed filtering antenna and its application for wearable devices with low SAR," *IEEE Trans. Antennas Propag.*, vol. 63, no. 9, pp. 3808–3818, Sep. 2015.

[111] X. Y. Zhang, W. Duan, and Y.-M. Pan, "High-gain filtering patch antenna without extra circuit," *IEEE Trans. Antennas Propag.*, vol. 63, no. 2, pp. 5883–5888, Feb. 2015.

[112] J. F. Zhang, Y. J. Cheng, Y. R. Ding, and C. X. Bai, "A dual-band shared-aperture antenna with large frequency ratio, high aperture reuse efficiency, and high channel isolation," *IEEE Trans. Antennas Propag.*, vol. 67, no. 2, pp. 853–860, Feb. 2019.

[113] T. Li and Z. N. Chen, "Shared-surface dual-band antenna for 5G applications," *IEEE Trans. Antennas Propag.*, vol. 68, no. 2, pp. 1128–1133, Feb. 2020.

[114] J. Lan, Z. Yu, J. Zhou, and W. Hong, "An aperture-sharing array for (3.5, 28) GHz terminals with steerable beam in millimeter-wave band," *IEEE Trans. Antennas Propag.*, vol. 68, no. 5, pp. 4114–4119, May 2020.

[115] Y. Liu, Y. Li, L. Ge, J. Wang, and B. Ai, "A compact hepta-band mode-composite antenna for sub (6, 28, and 38) GHz applications," *IEEE Trans. Antennas Propag.*, vol. 68, no. 4, pp. 2593–2602, Apr. 2020.

[116] M. S. Sharawi, M. Ikram, and A. Shamim, "A two concentric slot loop based connected array MIMO antenna system for 4G/5G terminals," *IEEE Trans. Antennas Propag.*, vol. 65, no. 12, pp. 6679–6686, Dec. 2017.

[117] Y. P. Zhang and J. Mao, "An overview of the development of antenna-in-package technology for highly integrated wireless devices," *Proc. IEEE*, vol. 107, no. 11, pp. 2265–2280, Nov. 2019.

[118] Y. P. Zhang and D. Liu, "Antenna-on-chip and antenna-in-package solutions to highly integrated millimeter-wave devices for wireless communications," *IEEE Trans. Antennas Propag.*, vol. 57, no. 10, pp. 2830–2841, Oct. 2009.

[119] W. Hong, K. H. Baek, and A. Goudelev, "Grid assembly-free 60-GHz antenna module embedded in FR-4 transceiver carrier board," *IEEE Trans. Antennas Propag.*, vol. 61, no. 4, pp. 1573–1580, Apr. 2013.

[120] D. Liu, J. A. G. Akkermans, H.-C. Chen, and B. Floyd, "Packages with integrated 60-GHz aperture-coupled patch antennas," *IEEE Trans. Antennas Propag.*, vol. 59, no. 10, pp. 3607–3616, Oct. 2011.

[121] D. Liu, X. Gu, C. W. Baks, and A. Valdes-Garcia, "Antenna-in-package design considerations for Ka-band 5G communication applications," *IEEE Trans. Antennas Propag.*, vol. 65, no. 12, pp. 6372–6379, Dec. 2017.

[122] X. Gu *et al.*, "Development, implementation, and characterization of a 64-Element dual-polarized phased-array antenna module for 28-GHz high-speed data communications," *IEEE Trans. Microw. Theory Techn.*, vol. 67, no. 7, pp. 2975–2984, Jul. 2019.

[123] E. Degirmenci, "EMF test report: Ericsson AIR 5121," Ericsson AB, Stockholm, Sweden, Tech. Rep. GFTB-17:001589, Jan. 2018.

[124] Y. Aslan, C. E. Kiper, A. J. van den Biggelaar, U. Johannsen, and A. Yarovoy, "Passive cooling of mm-wave active integrated 5G base station antennas using CPU heatsinks," *Proc. 16th EuRAD*, Paris, France, Oct. 2019, pp. 121–124.

[125] J. Park, H. Seong, Y. N. Whang, and W. Hong, "Energy-efficient 5G phased arrays incorporating vertically polarized endfire planar folded slot antenna for MMWave mobile terminals," *IEEE Trans. Antennas Propag.*, vol. 68, no. 1, pp. 230–241, Jan. 2020.

[126] C.-F. Huang and L. Chen, "Realization of printed-on-display antenna for mobile terminals," *Electron. Lett.*, vol. 38, no. 20, pp. 1162–1163, Sep. 2002.

[127] H. J. Song, T. Y. Hsu, D. F. Sievenpiper, H. P. Hsu, J. Schaffner, and E. Yasan, "A method for improving the efficiency of transparent film antennas," *IEEE Antennas Wireless Propag. Lett.*, vol. 7, pp. 753–756, 2008.

[128] F. Colombel, X. Castel, M. Himdi, G. Legeay, S. Vigneron, and E. M. Cruz, "Ultrathin metal layer, ITO film and ITO/Cu/ITO multilayer towards transparent antenna," *IET Sci. Meas. Technol.*, vol. 3, no. 3, pp. 229–234, May 2009.

[129] J. Park, S. Y. Lee, J. Kim, D. Park, W. Choi, and W. Hong, "An optically invisible antenna-on-display concept for millimeter-wave 5G cellular devices," *IEEE Trans. Antennas Propag.*, vol. 67, no. 5, pp. 2942–2952, May 2019.

[130] NR; Base Station (BS) Conformance Testing Part 2: Radiated Conformance Testing (Release 16), document 3GPP TS 38.141-2, 2019.

[131] NR; User Equipment (UE) Conformance Specification; Radio Transmission and Reception; Part 2: Range 2 Standalone (Release 16), document 3GPP TS 38.521-2, 2019.

[132] E. G. Larsson, O. Edfors, F. Tufvesson, and T. L. Marzetta, "Massive MIMO for next generation wireless systems," *IEEE Commun. Mag.*, vol. 52, no. 2, pp. 186–195, Feb. 2014.

[133] K. T. Selvan and R. Janaswamy, "Fraunhofer and Fresnel distances: Unified derivation for aperture antennas," *IEEE Antennas Propag. Mag.*, vol. 59, no. 4, pp. 12–15, Aug. 2017.

[134] S. Mano and T. Katagi, "A method for measuring amplitude and phase of each radiating element of a phased array antenna," *Trans. IECE*, vol. J65-B, no. 5, pp. 555–560, May 1982.

[135] T. Takahashi, H. Miyashita, Y. Konishi, and S. Makino, "Theoretical study on measurement accuracy of rotating element electric field vector (REV) method," *Commun. Jpn.*, vol. 90, no. 1, pp. 22–33, 2006.

[136] Y. Yu, W. Hong, Z. H. Jiang, H. Zhang, and C. Guo, "Multi-beam generation and measurement of a DDS-based digital beam-forming array transmitter at Ka-band," *IEEE Trans. Antennas Propag.*, vol. 67, no. 5, pp. 3030–3039, Jan. 2019.

[137] T. Takahashi *et al.*, "Fast measurement technique for phased array calibration," *IEEE Trans. Antennas Propag.*, vol. 56, no. 7, pp. 1888–1899, Jul. 2008.

[138] T. Takahashi *et al.*, "A novel amplitude-only measurement method to determine element fields in phased arrays," *IEEE Trans. Antennas Propag.*, vol. 60, no. 7, pp. 3222–3230, Jul. 2012.

[139] S. D. Silverstein, "Application of orthogonal codes to the calibration of active phased array antennas for communication satellites," *IEEE Trans. Signal Process.*, vol. 45, no. 1, pp. 206–218, Jan. 1997.

[140] R. Long, J. Ouyang, F. Yang, W. Han, and L. Zhou, "Multi-element phased array calibration method by solving linear equations," *IEEE Trans. Antennas Propag.*, vol. 65, no. 6, pp. 2931–2939, Jun. 2017.

[141] H. Yang, J. Jang, T. Sun, K. Kim, and S. Choi, "Calibration method using the zadoff-chu sequence," in *Proc. Int. Conf. ICT Convergence*, Jeju, South Korea, Dec. 2013, pp. 319–324.

[142] S. Qin, X. Ma, and W. Sheng, "Design and measurement of channel calibration for digital array with orthogonal codes," in *Proc. Int. Conf. Microw. Millimeter Wave Technol.*, Shenzhen, China, May 2012, pp. 1–4.
[143] S. Park, H.-S. Lee, and J.-G. Yook, "Orthogonal code-based transmitted radiation pattern measurement method for 5G massive MIMO antenna systems," *IEEE Trans. Antennas Propag.*, vol. 68, no. 5, pp. 4007–4013, May 2020.
[144] S. Smith *et al.*, "A millimeter-wave antenna amplitude and phase measurement system," *IEEE Trans. Antennas Propag.*, vol. 60, no. 4, pp. 1744–1756, Apr. 2012.
[145] Y. Hu, S. Wang, and S. An, "Over the air testing and error analysis of 5G active antenna system base station in compact antenna test range," in *Proc. Photon. Electromagn. Res. Symp. Fall*, Xiamen, China, Dec. 2019, pp. 1–4.
[146] S. F. Gregson and C. G. Parini, "Use of OTA system performance metrics in the design and optimization of CATRs for 5G testing," in *Proc. Antenna Meas. Technol. Assoc.*, San Diego, CA, USA, Oct. 2019, pp. 1–5.
[147] J. J. Lee, E. M. Ferrer, D. P. Woollen, and K. M. Lee, "Near-field probe used as a diagnostic tool to locate defective elements in an array antenna," *IEEE Trans. Antennas Propag.*, vol. AP-36, no. 3, pp. 884–889, Jun. 1988.
[148] R. Long, J. Ouyang, F. Yang, Y. Li, K. Zhang, and L. Zhou, "Calibration method of phased array based on near-field measurement system," in *Proc. IEEE Antennas Propag. Soc. Int. Symp.*, Memphis, TN, USA, Jul. 2014, pp. 1161–1162.
[149] J. Lundgren *et al.*, "A near-field measurement and calibration technique: Radio-frequency electromagnetic field exposure assessment of millimeter-wave 5G devices," *IEEE Antennas Propag. Mag.*, early access, doi: 10.1109/TAP.2020.2988517.
[150] G. F. Hamberger, C. Rowell, and B. Derat, "Near-field techniques for millimeter-wave antenna array calibration," in *Proc. Antenna Meas. Technol. Assoc.*, San Diego, CA, USA, Oct. 2019, pp. 1–5.
[151] D. Novotny *et al.*, "Performance evaluation of a robotically controlled millimeter-wave near-field pattern range at the NIST," in *Proc. 7th Eur. Conf. Antennas Propag.*, Gothenburg, Sweden, Apr. 2013, pp. 4086–4089.
[152] A. Yaghjian, "An overview of near-field antenna measurementss," *IEEE Trans. Antennas Propag.*, vol. 34, no. 1, pp. 30–45, Jan. 1986.
[153] S. F. Razavi and Y. Rahmat-Samii, "A new look at phaseless planar near-field measurements: Limitations, simulations, measurements, and a hybrid solution," *IEEE Antennas Propag. Mag.*, vol. 49, no. 2, pp. 170–178, 2007.
[154] A. Capozzoli, C. Curcio, G. D'Elia, and A. Liseno, "Millimeter-wave phaseless antenna characterization," *IEEE Trans. Instrum. Meas.*, vol. 57, no. 7, Jul. 2008.
[155] S. Costanzo, G. Di Massa, and M. D. Migliore, "A novel hybrid approach for far-field characterization from near-field amplitude-only measurements on arbitrary scanning surfaces," *IEEE Trans. Antennas Propag.*, vol. 53, no. 6, pp. 1866–1874, Jun. 2005.
[156] O. M. Bucci, G. D'Elia, G. Leone, and R. Pierri, "Far field pattern determination from the near-field amplitude on two surfaces," *IEEE Trans. Antennas Propag.*, vol. 38, no. 11, pp. 1771–1779, Nov. 1990.
[157] R. Pierri, G. D'Elia, and F. Soldovieri, "A two probes scanning phaseless near-field far-field transformation technique," *IEEE Trans. Antennas Propag.*, vol. 47, no. 5, pp. 792–802, May 1999.
[158] H. Kong, Y. Jing, Z. Wen, and M. Yau, "A compact millimeter wave (MMWave) mid-field over the air (OTA) RF performance test system for 5G massive MIMO devices," in *Proc. MTT-S Int. Wireless Symp.*, Chengdu, China, May 2018, pp. 1–4.
[159] H. Kong, Z. Wen, Y. Jing, and M. Yau, "Midfield over-the-air test: A new OTA RF performance test method for 5G massive MIMO devices," *IEEE Trans. Microw. Theory Techn.*, vol. 67, no. 7, pp. 2873–2883, Jul. 2019.
[160] M. A. Salas-Natera, R. M. Rodriguez-Osorio, and L. Haro, "Procedure for measurement, characterization, and calibration of active antenna arrays," *IEEE Trans. Instrum. Meas.*, vol. 62, no. 2, pp. 377–391, Feb. 2013.
[161] D. Kim, S. Park, T. Kim, L. Minz, and S. Park, "Fully digital beamforming receiver with a real-time calibration for 5G mobile communication," *IEEE Trans. Antennas Propag.*, vol. 67, no. 6, pp. 3809–3819, Jun. 2019.
[162] H. M. Aumann, A. J. Fenn, and F. G. Willwerth, "Phased array antenna calibration and pattern prediction using mutual coupling measurements," *IEEE Trans. Antennas Propag.*, vol. 37, no. 7, pp. 844–850, Jul. 1989.
[163] C. Shipley and D. Woods, "Mutual coupling-based calibration of phased array antennas," in *Proc. IEEE Int. Conf. Phased Array Syst. Technol.*, Dana Point, CA, USA, May 2000, pp. 529–532.
[164] R. S. Chu and K. M. Lee, "Analysis and development of signal injection technique using transmission lines embedded at phased array aperture," in *IEEE Antennas Propag. Soc. Int. Symp. Dig.*, Chicago, IL, USA, Jun. 1992, pp. 433–436.
[165] K. M. Lee, R. S. Chu, and S. C. Liu, "A built-in performance monitoring/fault isolation and correction (PM/FIC) system for active phased array antennas," in *Proc. IEEE Antennas Propag. Soc. Int. Symp.*, Ann Arbor, MI, USA, Jun.- Jul. 1993, pp. 206–209.
[166] M. E. Leinonen, M. Jokinen, N. Tervo, O. Kursu, and A. Pärssinen, "System EVM characterization and coverage area estimation of 5G directive MMW links," *IEEE Trans. Microw. Theory Techn.*, vol. 67, no. 12, pp. 5282–5295, Dec. 2019.
[167] C. Guo, Y. Hu, Z. B. Jiang, and W. Hong, "Investigations on OTA calibration and test method in 5G millimeter wave base station," *J. Microwave (in Chinese)*, vol. 35, no. 6, pp. 72–76, Dec. 2019.
[168] NR; Study on test methods (Release 16), document 3GPP TS 38.810, 2019.
[169] A. Scannavini, F. Saccardi, L. J. Foged, and K. Zhao, "Impact of phase curvature on measuring 5G millimeter wave devices," in *Proc. Antenna Meas. Technol. Assoc.*, San Diego, CA, USA, Oct. 2019, pp. 1–4.
[170] V. Rodriguez, "Basic rules for anechoic chamber design, part two: Compact ranges and near field measurements," *Microw. J.*, vol. 59, no. 2, pp. 80–90, Jan. 2016.
[171] C. Rowell and A. Tankielun, "Plane wave converter for 5G massive MIMO basestation measurements," in *Proc. 12th Eur. Conf. Antennas Propag.*, London, U.K., Apr. 2018, pp. 1–3.
[172] Rohde & Schwarz Co., "R&S PWC200 plane wave converter for 5G massive MIMO base station testing." [Online]. Available: https://www.rohde-schwarz.com/tw/product/pwc200-productstartpage_63493-533696.html?rusprivacypolicy=0
[173] Z. Jiang, W. Hong, N. Zhang, and C. Yu, "Progress and challenges of test technolgies for 5G," *Microw. J.*, vol. 61, no. 1, pp. 80–94, Jan. 2018.
[174] P.-S. Kildal and K. Rosengren, "Correlation and capacity of MIMO systems and mutual coupling, radiation efficiency, and diversity gain of their antennas: Simulations and measurements in a reverberation chamber," *IEEE Commun. Mag.*, vol. 42, no. 12, pp. 104–112, Dec. 2004.
[175] S.-J. Park *et al.*, "Performance comparison of 2 $\times$ 2 MIMO antenna arrays with different configurations and polarizations in reverberation chamber at millimeter-wave band," *IEEE Trans. Antennas Propag.*, vol. 65, no. 12, pp. 6669–6678, Dec. 2017.
[176] R. Aminzadeh *et al.*, "Estimation of average absorption cross section of a skin phantom in a mm-Wave reverberation chamber," in *Proc. 13th Eur. Conf. Antennas Propag.*, Krakow, Poland, Mar./Apr. 2019, pp. 1–3.
[177] P. Zhang, X. Yang, J. Chen, and Y. Huang, "A survey of testing for 5G: Solutions, opportunities, and challenges," *China Commun.*, vol. 16, no. 1, pp. 69–85, Jan. 2019.
[178] Y. Jing, X. Zhao, H. Kong, S. Duffy, and M. Rumney, "Two-stage over the air (OTA) test method for LTE MIMO device performance evaluation," in *Proc. Int. Symp. Antennas Propag.*, Spokane, WA, USA, Jul. 2011, pp. 1–4.
[179] 3GPP, Verification of Radiated Multi-Antenna Reception Performance of User Equipment (Release 16), document 3GPP TR 37.977, 2019.
[180] M. Rumney, H. Kong, and Y. Jing, "Practical active antenna evaluation using the two-stage MIMO OTA measurement method," in *Proc. 8th Eur. Conf. Antennas Propag.*, The Hague, Netherlands, Apr. 2014, pp. 3500–3503.
[181] H. Q. Gao *et al.*, "Over-the-Air testing for carrier aggregation enabled MIMO terminals using radiated two-stage method," *IEEE Access*, vol. 6, pp. 71622–71631, Dec. 2018.
[182] CTIA, Test Plan for 2 $\times$ 2 Downlink MIMO and Transmit Diversity Over-the-Air Performance, CTIA Tech. Rep. Version 1.1.1, Apr. 2017.
[183] Y. Ji, W. Fan, G. F. Pedersen, and X. Wu, "On channel emulation methods in multiprobe anechoic chamber setups for over-the-air eesting," *IEEE Trans. Veh. Technol.*, vol. 67, no. 8, pp. 6740–6751, Aug. 2018.

[184] W. Fan, P. Kyosti, M. Rumney, X. Chen, and G. F. Pedersen, "Over-the-air radiated testing of millimeter-wave beam-steerable devices in a cost-effective measurement setup," *IEEE Commun. Mag.*, vol. 56, no. 7, pp. 64–71, Jul. 2018.

[185] H. Pei, X. Chen, M. Zhang, and A. Zhang, "Over-the-air testing of 5G millimeter-wave system with adaptive beamforming," in *Proc. MTT-S Int. Wireless Symp.*, Guangzhou, China, May 2019, pp. 1–3.

[186] Z. B. Jiang, C. Guo, and W. Hong, "Research and progress in 5G millimeter wave testing: An overview," *Bull. Nat. Natural Sci. Found. China*, vol. 34, no. 2, pp. 126–132, 2020.

[187] Y. Li, L. Xin, X. Liu, and X. Zhang, "Dual anechoic chamber setup for over-the-air radiated testing of 5G devices," *IEEE Trans. Antennas Propag.*, vol. 68, no. 3, pp. 2469–2474, Mar. 2020.

[188] M. Shafi *et al.*, "Microwave vs. millimeter-wave propagation channels: Key differences and impact on 5G cellular systems," *IEEE Commun. Mag.*, vol. 56, no. 12, pp. 14–20, Dec. 2018.

[189] T. S. Rappaport, G. R. MacCartney, M. K. Samimi, and S. Sun, "Wideband millimeter-wave propagation measurements and channel models for future wireless communication system design," *IEEE Trans. Commun.*, vol. 63, no. 9, pp. 3029–3056, Sep. 2015.

[190] H. Wang, P. Zhang, J. Li, and X. You, "Radio propagation and wireless coverage of LSAA-based 5G millimeter-wave mobile communication systems," *China Commun.*, vol. 16, no. 5, pp. 1–18, May 2019.

[191] C.-X. Wang, S. Wu, L. Bai, X. You, J. Wang, and C.-L. I, "Recent advances on massive MIMO channel measurements and modeling: A survey," *Sci. China Inf. Sci.*, vol. 59, no. 2, Feb. 2016.

[192] P. Zhang, B. Yang, C. Yi, H. Wang, and X. You, "Measurement-based 5G millimeter-wave propagation characterization in vegetated suburban macrocell environments," *IEEE Trans. Antennas Propag.*, vol. 68, no. 7, pp. 5556–5567, Jul. 2020.

[193] I. A. Hemadeh, K. Satyanarayana, M. El-Hajjar, and L. Hanzo, "Millimeter-wave communications: Physical channel models, design considerations, antenna constructions, and link-budget," *IEEE Commun. Surveys Tuts.*, vol. 20, no. 2, pp. 870–913, 2nd-quarter 2018.

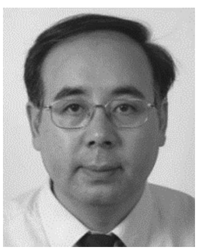

WEI HONG (Fellow, IEEE) received the B.S. degree from the University of Information Engineering, Zhengzhou, China, in 1982, and the M.S. and Ph.D. degrees from Southeast University, Nanjing, China, in 1985 and 1988, respectively, all in radio engineering.

He has been with the State Key Laboratory of Millimeter Waves, Southeast University, since 1988, where he has also been the Director of the Laboratory since 2003. He is currently a Professor of the School of Information Science and Engineering with Southeast University. In 1993 and 1995–1998, he was a short-term Visiting Scholar with the University of California at Berkeley and at Santa Cruz, CA, USA, respectively. He has authored or coauthored over 300 technical publications and authored two books. His current research interests include numerical methods for electromagnetic problems, millimeter-wave theory and technology, antennas, electromagnetic scattering, and RF technology for mobile communications

Prof. Hong was an elected IEEE MTT-S AdCom Member from 2014 to 2016. He is a Fellow of CIE. He was twice awarded the National Natural Prizes, and thrice awarded the First-Class Science and Technology Progress Prizes issued by the Ministry of Education of China and Jiangsu Province Government. He also received the Foundations for China Distinguished Young Investigators and for "Innovation Group" issued by the NSF of China. He is the Vice President of the CIE Microwave Society and Antenna Society and the Chair of the IEEE MTTS/APS/EMCS Joint Nanjing Chapter. He served as an Associate Editor of IEEE TRANSACTIONS ON MICROWAVE THEORY AND TECHNIQUES from 2007 to 2010, and was one of the Guest Editors for the 5G special issue of IEEE TRANSACTIONS ON ANTENNAS AND PROPAGATION in 2017.

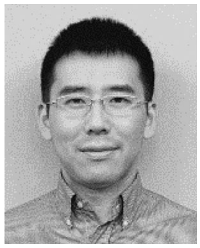

ZHI HAO JIANG (Member, IEEE) received the B.S. degree in radio engineering from Southeast University, Nanjing, in 2008, and the Ph.D. degree in electrical engineering from The Pennsylvania State University, University Park, State College, PA, USA, in 2013. From 2013 to 2016, he was a Postdoctoral Fellow with the Computational Electromagnetics and Antennas Research Laboratory, Department of Electrical Engineering, The Pennsylvania State University. He is currently a Professor with the State Key Laboratory of Millimeter Waves, School of Information Science and Engineering, Southeast University. Dr. Jiang has authored or co-authored about 90 papers in peer-reviewed journals, more than 70 papers in conference proceedings, as well as eight book chapters. He has also co-edited one book *Electromagnetics of Body-Area Networks: Antennas, Propagation, and RF Systems* (Wiley/IEEE Press, 2016) and coauthored eight book chapters. He holds seven granted U.S. patents and eight granted Chinese patents. His current research interests include microwave/millimeter-wave antennas and circuits, millimeter-wave systems, impedance surfaces, metamaterials, and analytical methods. He was the recipient of the URSI Young Scientist Award in 2020, the 2019 ACES-China Young Scientist Award, the High-Level Innovative and Entrepreneurial Talent presented by Jiangsu Province, China, in 2017, the Thousands of Young Talents presented by China government in 2016, the 2012 A. J. Ferraro Outstanding Doctoral Research Award in Electromagnetics, and the Best (Student) Paper Awards at several international conferences. He is an Associate Editor for *IET Communications*, and was a Guest Editor of *International Journal of RF and Microwave Computer-Aided Engineering*.

CHAO YU (Member, IEEE) received the B.E. degree in information engineering and the M.E. degree in electromagnetic fields and microwave technology from Southeast University (SEU), Nanjing, China, in 2007 and 2010, respectively, and the Ph.D. degree in electronic engineering from University College Dublin (UCD), Dublin, Ireland, in 2014. He is currently an Associate Professor with the State Key Laboratory of Millimeter Waves, School of Information Science and Engineering, Southeast University. His research interests include microwave and millimeter wave power amplifier modeling and linearization, and 5G massive MIMO RF system design.

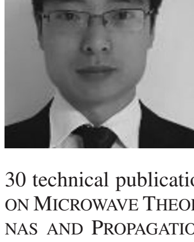

DEBIN HOU received the B.S. degree from the University of Electronic Science and Technology of China (UESTC), Chengdu China, and the Ph.D. degree from Southeast University (SEU), Nanjing China in 2007 and 2013, respectively. He was an exchange student at the Institute of Microelectronics (IME), A*STAR, Singapore, and the Blekinge Institute of Technology (BTH), Sweden. He is currently an Associate Professor with the State Key Laboratory of Millimeter Waves, Southeast University. He has authored and coauthored more than 30 technical publications in several journals including IEEE TRANSACTIONS ON MICROWAVE THEORY AND TECHNIQUES, IEEE TRANSACTIONS ON ANTENNAS AND PROPAGATION, etc. His current research interests include silicon-based/GaAs millimeter-wave/THz on-chip components, antennas and integrated circuits. He was the recipient of the "Jiangsu Excellent 100 Doctoral Dissertation" prize in 2014.

HAIMING WANG (Member, IEEE) was born in 1975. He received the B.S., M.S., and Ph.D. degrees in electrical engineering from Southeast University, Nanjing, China, in 1999, 2002, and 2009, respectively.

In April 2002, he joined the State Key Laboratory of Millimeter Waves, Southeast University, where he is currently a Professor. In 2008, he was a short-term Visiting Scholar with the Blekinge Institute of Technology, Sweden. His current research interests include millimeter-wave wireless mobile communications, millimeter-wave radar and imaging, radio propagation measurement and channel modeling, multi-band and broadband antennas and arrays. He has authored and coauthored more than 50 technical publications in IEEE Transactions on Antennas and Propagation, IEEE Antennas Wireless Propagation Letters, and other peer-reviewed academic journals. He has authored and coauthored more than 60 patents and 52 patents have been granted.

Dr. Wang was the recipient of the First-Class Science and Technology Progress Award of Jiangsu Province of China in 2009. He was the Vice Chair of IEEE 802.11aj Task Group from September 2012 to July 2018. He was awarded for contributing to the development of IEEE 802.11aj by the IEEE-SA in July 2018.

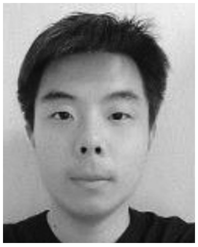

CHONG GUO (Graduate Student Member, IEEE) was born in Zhengzhou, Henan, China, in 1992. He received the B.S. degree in electronic engineering from the University of Electronic Science and Technology of China, Chengdu, China, in 2015. He is currently working toward the Ph.D. degree in microwave technology with the State Key Laboratory of Millimeter Waves, Southeast University, Nanjing, China. His current research interests include microwave and millimeter-wave massive MIMO system design and measurement.

Mr. Guo was the recipient of the Best Student Paper Award in the 2019 IEEE MTT-S International Wireless Symposium.

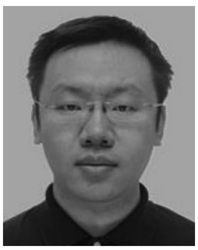

YUN HU (Member, IEEE) was born in Taigu, Shanxi province, China, 1986. He received the B.Eng. degree in electronics and information engineering and the M.Eng. degree in circuits and systems from the University of Electronic Science and Technology of China, Chengdu, China, in 2008 and 2011, respectively, and the Ph.D. degree in electromagnetic and microwave engineering from Southeast University, Nanjing, China, in 2019. From July 2011 to February 2015, he was with the Second Academy of China Aerospace Science and Industry Corporation, Beijing, as a Research Engineer. He is currently a Researcher with Purple Mountain Laboratories, Nanjing, China. His current research interests include multibeam antennas, antenna arrays, beamforming networks, and radio frequency (RF) front-end design.

Dr. Hu was the recipient of the Student Paper Award of the 2018 IEEE 7th Asia-Pacific Conference on Antennas and Propagation (APCAP 2018).

LE KUAI was born in Nanjing, Jiangsu, China, in 1990. He received the B.S. degree in electronic information engineering from Southeast University Chengxian College, Nanjing, China, in 2012 and the M.S. degree in microelectronics and solid state electronics from Nanjing Electronic Devices Institute, Nanjing, China, in 2015. He is currently working toward the Ph.D. degree in electromagnetic field and microwave technology with Southeast University. His research interests include microwave circuits and 5th generation of mobile communication.

YINGRUI YU (Member, IEEE) was born in Nanjing, China, in 1992. He received the B.S. degree in communication engineering from the Nanjing University of Science and Technology (NJUST), Nanjing, China, in 2014 and the Ph.D. degree in microwave technology from the State Key Laboratory of Millimeter Waves, Southeast University, Nanjing, China, in 2020. From 2018 to 2019, he was an Honorary Associate with the Department of Electrical and Computer Engineering (ECE), University of Wisconsin–Madison, Madison, WI, USA. He has authored several journal papers in IEEE Transactions on Antennas and Propagation. His current research interests include antenna array theory and design, millimeter-wave radar, and communication system. Mr. Yu was the recipient of the Scholarship from the China Scholarship Council. He is also thrice awarded the National Scholarship for Undergraduate Students issued by the Ministry of Education of China, from 2011 to 2013. He is a reviewer of IEEE Transactions on Communications, IEEE Access, *Electronic Letters*, and *AEU- International Journal of Electronics and Communications*.

ZHENGBO JIANG (Member, IEEE) received the B.S. degree from Radio Engineering Department, Southeast University in 2002, and the M.S. and Ph.D. degrees from Southeast University, Nanjing, China, in 2004 and 2009, respectively, all in electromagnetic field and microwave technology discipline. Since 2009, he has been with the State Key Laboratory of Millimeter Waves, and is currently an Associate Professor with the School of Information Science and Engineering, Southeast University. His major research focuses on key technologies of millimeter wave instruments, 5G/6G mobile communication testing, and MIMO wireless channel. As the Chief Scientist, he has led the completion of two Major National Science & Technology Specific Projects. He also participated in several national scientific research projects such as NSFC, and the national 863 projects. He has led the development of a series of measurement instruments, such as wireless scanners, channel emulators, and vector signal analyzers.

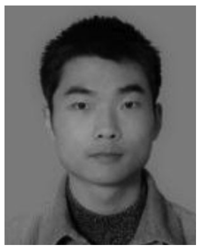

ZHE CHEN (Member, IEEE) received the B.S. degree in electronic information engineering from the University of Electronic Science and Technology of China, Chengdu, China, in 2006, and the Ph.D. degree in electromagnetic field and microwave technology from Southeast University, Nanjing, China, in 2014. Since 2014, he has been with the Sate Key Laboratory of Millimeter Waves, School of Information Science and Engineering, Southeast University. His research interests include design of millimeter-wave/THz wireless transceiver and frequency generations for wireless communications in nanometer CMOS technology.

JIXIN CHEN (Member, IEEE) was born in Jiangsu, China, in 1976. He received the B.S. degree in radio engineering and the M.S. and Ph.D. degrees in electromagnetic field and microwave technique from Southeast University, Nanjing, China, in 1998, 2002, and 2006, respectively.

Since 1998, he has been with the Sate Key Laboratory of Millimeter Waves, Southeast University, where he is currently a Professor with the School of Information Science and Engineering. He has authored or coauthored more than 100 papers and presented invited papers at ICMMT2016, IMWS2012, and GSMM2011. His current research interests include microwave and millimeter-wave circuit design and monolithic microwave integrated circuit design.

Dr. Chen was the recipient of the 2016 Keysight Early Career Professor Award and the Best Student Paper Award of ICUWB 2016. He was the Technical Program Committee Co-Chair of HSIC2012 and UCMMT2012, the LOC Co-Chair of APMC2015, the Session Co-Chair of iWAT2011, ISSSE2010, and APMC2007, and a reviewer for IEEE Transactions on Microwave Theory and Techniques and IEEE Microwave and Wireless Components Letters.

ZHIQIANG YU (Member, IEEE) received the B.S. degree from the Nanjing University of Science and Technology, Nanjing, China, in 2002, and the Ph.D. degree from Southeast University, Nanjing, in 2013. From 2002 to 2007, he was a Research Staff in airborne radar transmitter with the Nanjing Institute of Electronics, China Electronics Technology Group Corporation, Nanjing. He is currently a Lecturer with the School of Information Science and Engineering, Southeast University. His current research interests include microwave and millimeter-wave transceiver systems, beamforming networks, and phased arrays for mobile communication.

JIANFENG ZHAI (Member, IEEE) received the B.S. degree in radio engineering and the Ph.D. degree in electromagnetic field and microwave technology from Southeast University, Nanjing, China, in 2004 and 2009, respectively. He is currently with the School of Information Science and Engineering, Southeast University. His current research interests include digital signal processing, neural networks, nonlinear modeling, microwave circuits design, PA linearization, and embedded systems.

NIANZU ZHANG received the M.S. and Ph.D. degrees from Southeast University, Nanjing, China, in 2003 and 2012, respectively. He is currently an Associate Professor with the School of Information Science and Engineering, Southeast University. His current research interests include wireless channel measurement and emulation, channel modeling and simulation, and massive multiple-input multiple-output system for 5G mobile communications.

LING TIAN (Member, IEEE) received the B.Eng., M.S., and Ph.D. degrees in electromagnetic and microwave engineering from Southeast University, Nanjing, China, in 1999, 2003, and 2009, respectively. She is currently with the State Key Laboratory of Millimeter Waves, Southeast University, Nanjing, China. Her research interests include RF components, circuits, and systems.

FAN WU (Member, IEEE) was born in Jiangxi, China. He received the B.Eng and M.Eng degrees in electronic engineering from Beijing Jiaotong University, Beijing, China, in 2012 and 2015, respectively, and the Ph.D. degree in electronic engineering from City University of Hong Kong, Hong Kong, in 2018.

He is currently an Assistant Professor with the State Key Laboratory of Millimeter Waves, School of Information Science and Engineering, Southeast University, Nanjing, China. His current research interests include medium-to-high gain antennas and arrays, circularly polarized antennas, and antenna wideband techniques.

Dr. Wu was the recipient of the Honorable Mention at the student contest of the 2018 IEEE APS-URSI Conference and Exhibition held in Boston, USA.

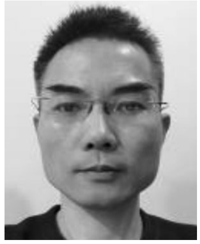

GUANGQI YANG received the B.S. degree in electronic engineering from the Nanjing University of Aeronautics and Astronautics, China, in 1995 and M.Sc. degree in electronic engineering from Southeast University, China, in 2002. From then on, he has been with Southeast University and focused on algorithm design as well as development of tools and prototypes to demonstrate innovative techniques for millimeter systems. His current research interests include joint design of RF and baseband subsystems, high-level synthesis, parallel computing, and continuous integration methodologies for FPGA-centric development.

ZHANG-CHENG HAO (Senior Member, IEEE) received the B.S. degree in microwave engineering from Xidian University, Xi'an, China, in 1997, and the M.S. and Ph.D. degrees in radio engineering from Southeast University, Nanjing, China, in 2002 and 2006, respectively. In 2006, he was a Postdoctoral Researcher with the Laboratory of Electronics and Systems for Telecommunications (LEST), École Nationale Supérieure des Télécommunications de Bretagne (ENSTB), Bretagne, France, where he was involved with developing millimeter-wave antennas. In 2007, he joined, as a Research Associate, the Department of Electrical, Electronic and Computer Engineering, Heriot-Watt University, Edinburgh, U.K., where he was involved with developing multilayer integrated circuits and ultrawide-band components. In 2011, he joined the School of Information Science and Engineering, Southeast University, Nanjing China, as a Professor. He holds 20 granted patents, and has authored and coauthored more than 200 referred technique papers. His current research interests include microwave and millimeter-wave systems, submillimeter-wave and terahertz components, and passive circuits, including filters, antenna arrays, couplers, and multiplexers. Dr. Hao was the TPC Chair/Co-Chair for many international conferences, such as iWat2018, ICMMT 2019, and ISAP 2019. He was a reviewer for many technique journals, including IEEE TRANSACTIONS ON MICROWAVE THEORY AND TECHNIQUES (IEEE T-MTT), IEEE TRANSACTIONS ON ANTENNAS AND PROPAGATION, IEEE ANTENNAS AND WIRELESS PROPAGATION LETTERS, and IEEE MICROWAVE AND WIRELESS COMPONENTS LETTERS, a Guest Editor for the IEEE T-MTT Special Issue on IWS 2018, and an Associate Editor for the *IET Electronics Letters* and *IET Microwaves Antennas, and Propagation*.

JIAN YI ZHOU (Member, IEEE) received the B.S.E.E., M.S.E.E., and Ph.D. degrees from Southeast University, Nanjing, China, in 1993, 1996, and 2001, respectively. In 1996, he joined the Faculty of the Department of Radio Engineering, Southeast University, as an Assistant Professor, and became a Lecturer in 1998, an Associate Professor in 2001, and a Professor in 2005. His current research interests include RF circuits and systems in mobile communications.